



Nanocomposite Coated Conductors

Towards optimal vortex pinning
for high field applications

Teresa Puig

Institut de Ciència de Materials de Barcelona,
ICMAB- CSIC, Bellaterra, Catalonia, Spain



T. Puig -EUCAS 2015

Acknowledgments



ICMAB-CSIC: X. Obradors, A. Palau, S. Ricart, M. Coll, J. Gázquez, E. Bartolomé, X. Granados, C. Pop, M. Tristany, P. Cayado, V. Rouco, R. Guzman, F. Vallès, B. Mundet, P. Garcés, H. Chen, L. Soler, B. Villarejo

EUROTAPES: J. Driscoll, R. Hühne, P. Pahlke, B. Holzapfel, J. Hänisch, G. Celentano, F. Rizzo, I. Van Driessche, K. Keukeleere, G. Van Tendeloo, A. Meledin, M. Eisterer, M. Lao

Bruker: A. Usoskin

D-Nano: M. Bäcker

Theva: M. Bauer, W. Pruseit

Oxolutia: A. Calleja

CERN: L. Bottura

SuperOx: A. Molodyk

University of Houston: V. Selvamanickam - **Superpower:** E. L. Keehan

University of Kansas: J. Wu

High Magnet Lab. Tallahassee: D. Larbalestier

AMSC: M. Rupich, S. Fleshler

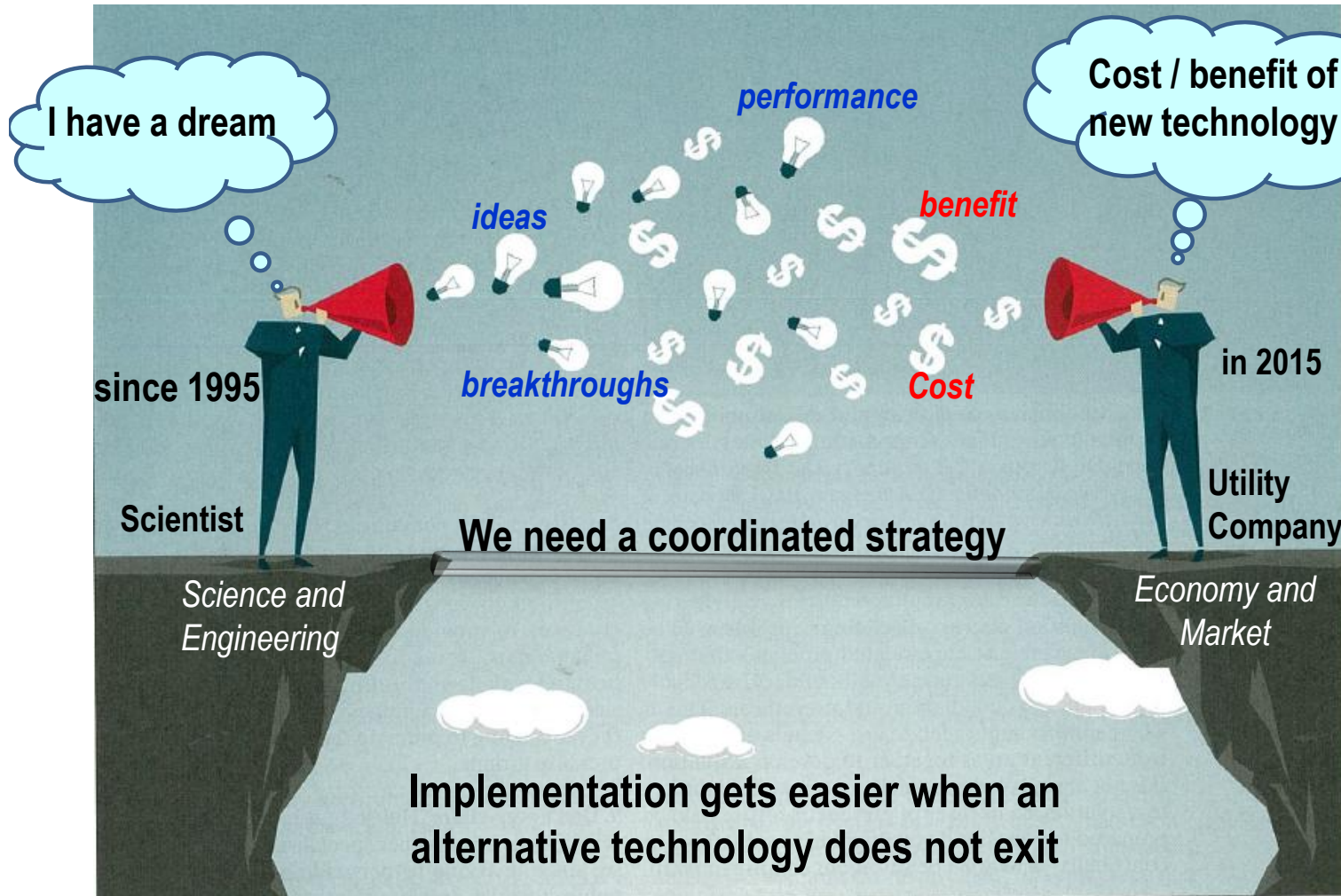
SuNAM: S. Moon

ISTEC: T. Izumi - **Kyushu Institute of Technology:** K. Matsumoto - **Hiroshima**

University : P. Mele - **Nagoya Univ. :** Y. Yoshida - **Fugikura:** Iijima - **Showa:** T.

Koizumi

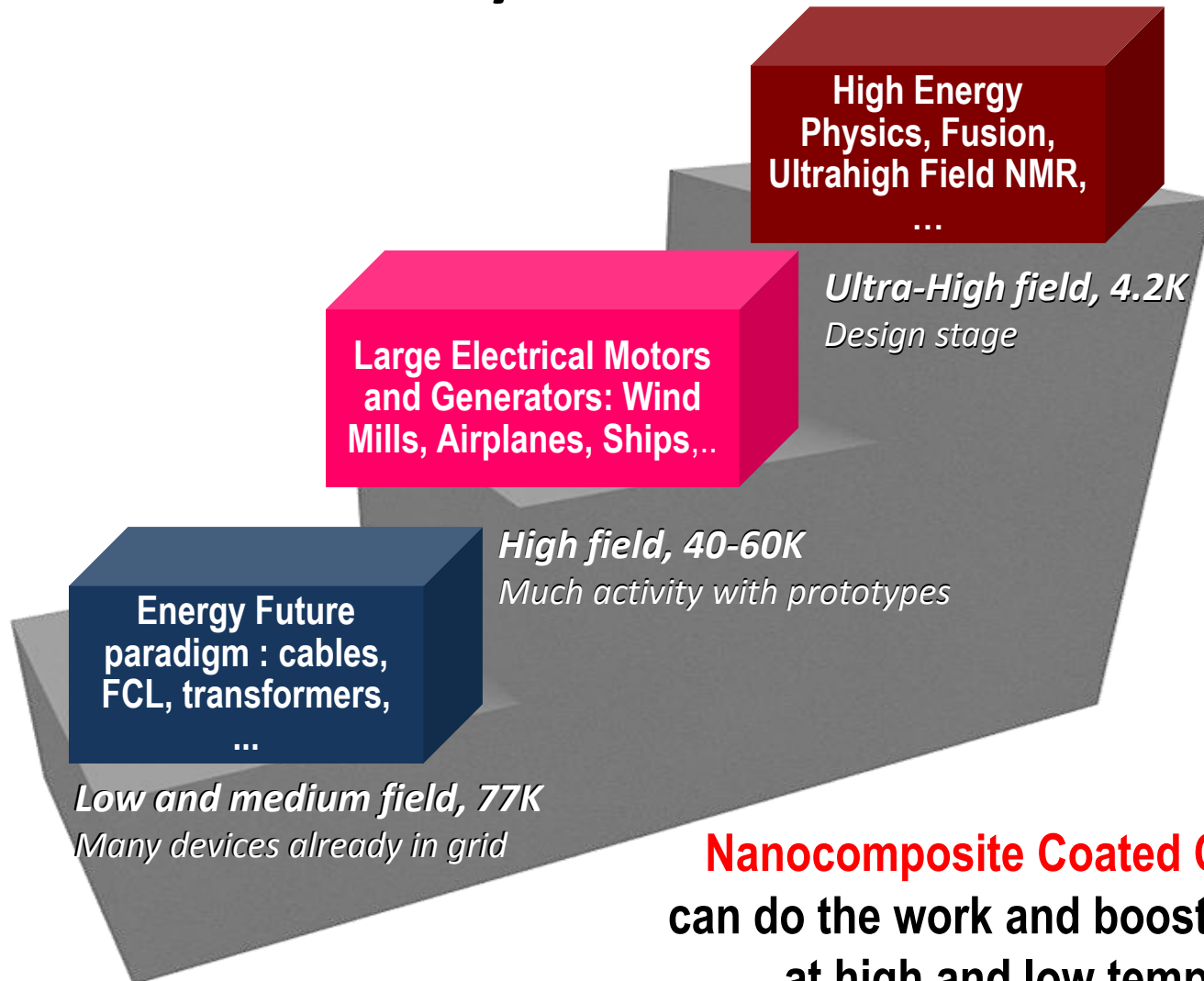
The World of Coated Conductors



Adapted from *Physcs World* August 2015

T. Puig -EUCAS 2015

The history of Coated Conductors



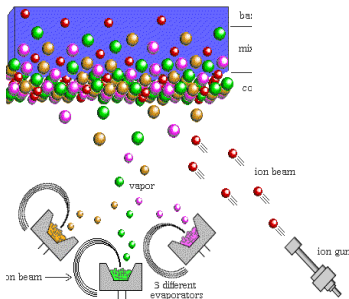


Coated Conductors are a revolution in materials science and engineering

started 15 years ago

*Multilayer epitaxial coatings
of high transport current*

**IBADs (ABAD): Ion
Beam Assisted
Deposited substrate**



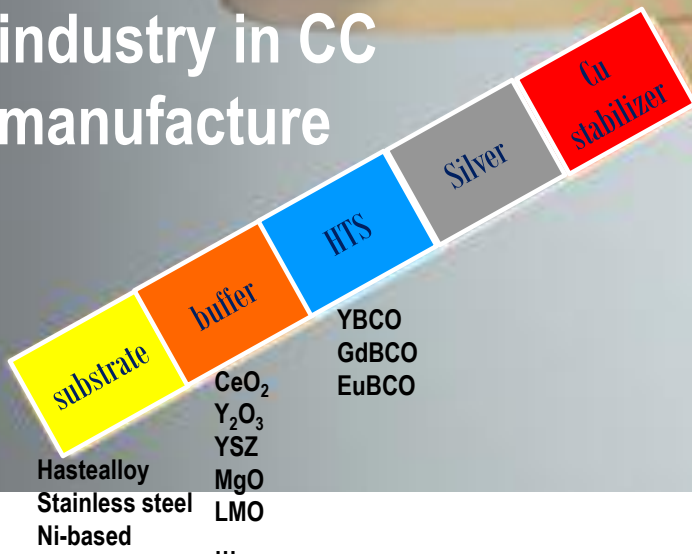
**RABiTs: Rolling
Assisted Biaxially
Textured substrate**



**... scalable technology for growing km-length epitaxial $(RE)Ba_2Cu_3O_7$
films on flexible metallic substrates**

Nowadays CC are ready for commercialization

We have a strong industry in CC manufacture

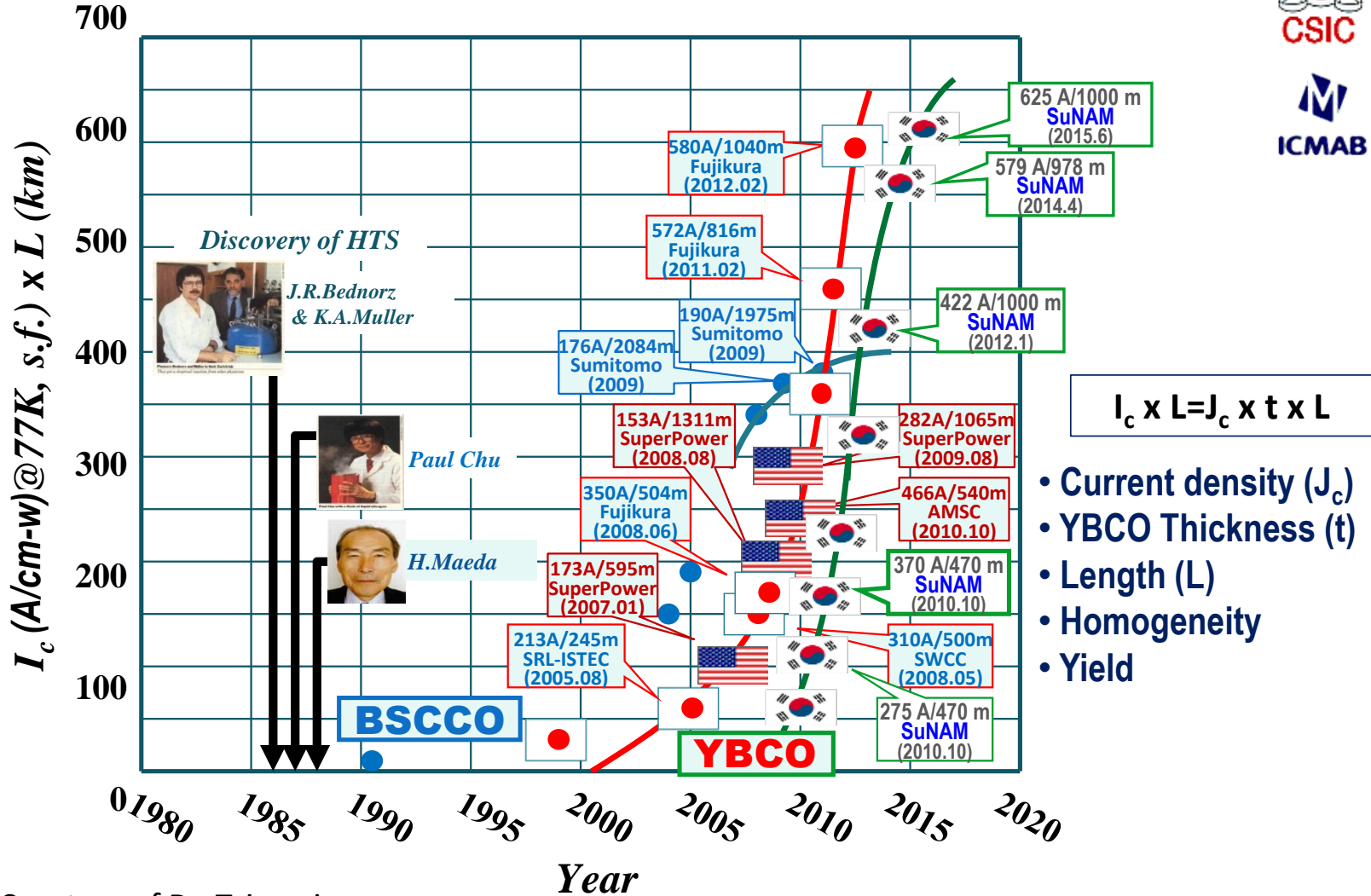


The Coated Conductor Tape





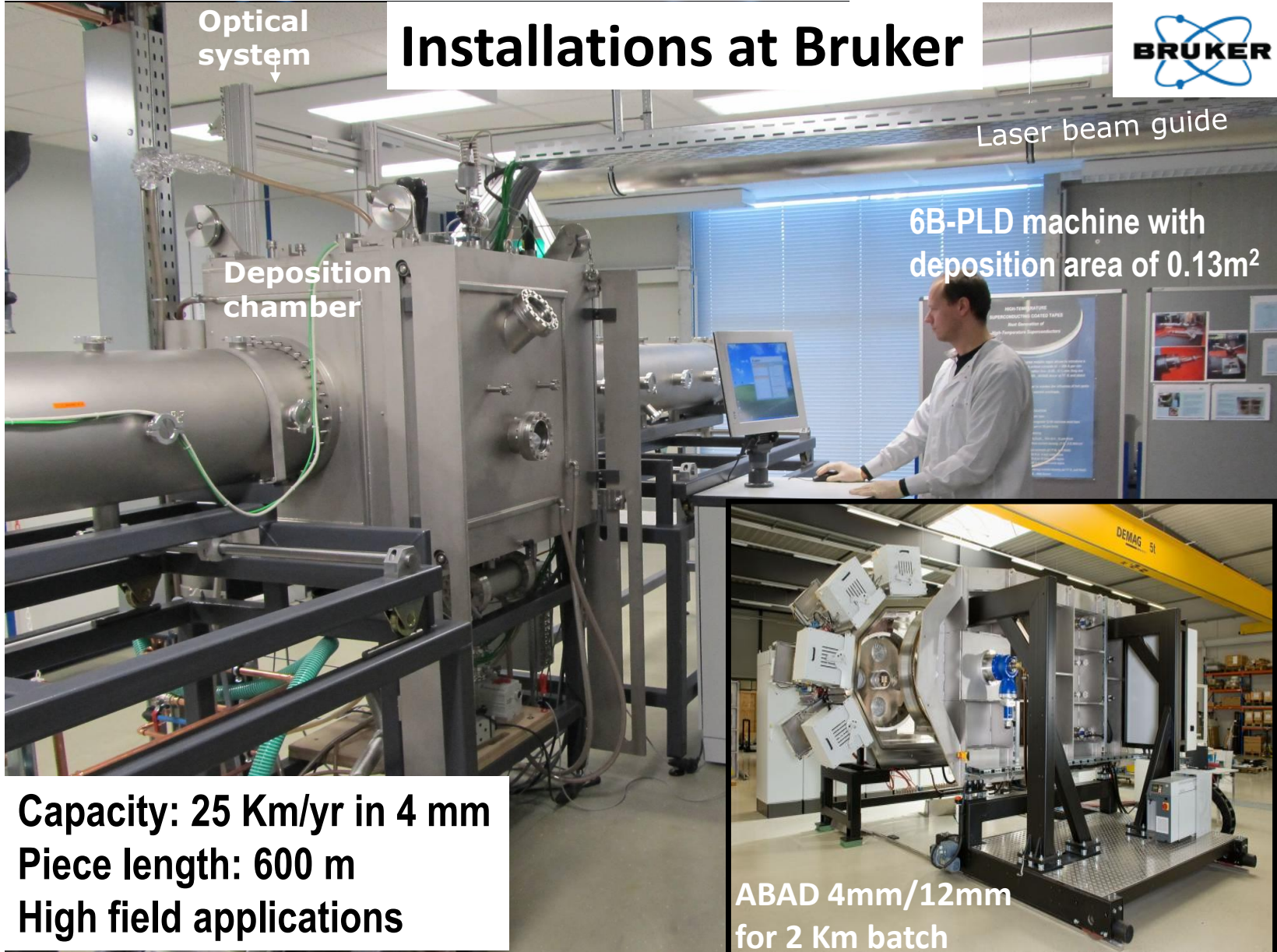
The huge progress of CC in the last 10 years



Courtesy of Dr. T. izumi

T. Puig -EUCAS 2015

Installations at Bruker



Optical system

Laser beam guide

Deposition chamber

6B-PLD machine with deposition area of 0.13m²

Capacity: 25 Km/yr in 4 mm
Piece length: 600 m
High field applications

ABAD 4mm/12mm
for 2 Km batch

2G superconducting tape by PVD PILOT PRODUCTION LINE

THEVA



**GdBCO evaporation
on ISD-MgO tape**

Min. processing speed: 30+ m/h
fully automated
inline quality inspection
reel-to-reel & air-to-air tape transfer

Piece length: 1 km

Capacity: 150 km/yr in 12 mm-width

T. Puig-EUCAS2015

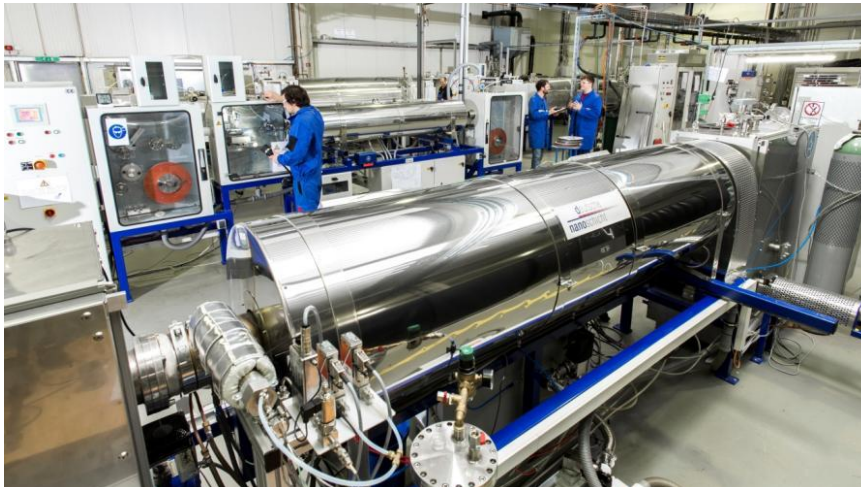
Expanded pilot line

- Construction in 2015
(Start sampling for customer projects in 2015/2016)
- **Planned capacity > 200 km/yr**
- **Present Length: 20 -100 m**

All CSD approach on RABiTs

$$I_c(77K,0T)/w = 294 \pm 5 \text{ A/cm}$$
$$I_c(30K,1T)/w = 853 \pm 5 \text{ A/cm}$$

HTS layer thickness $d = 1 \mu\text{m}$



Lab processing

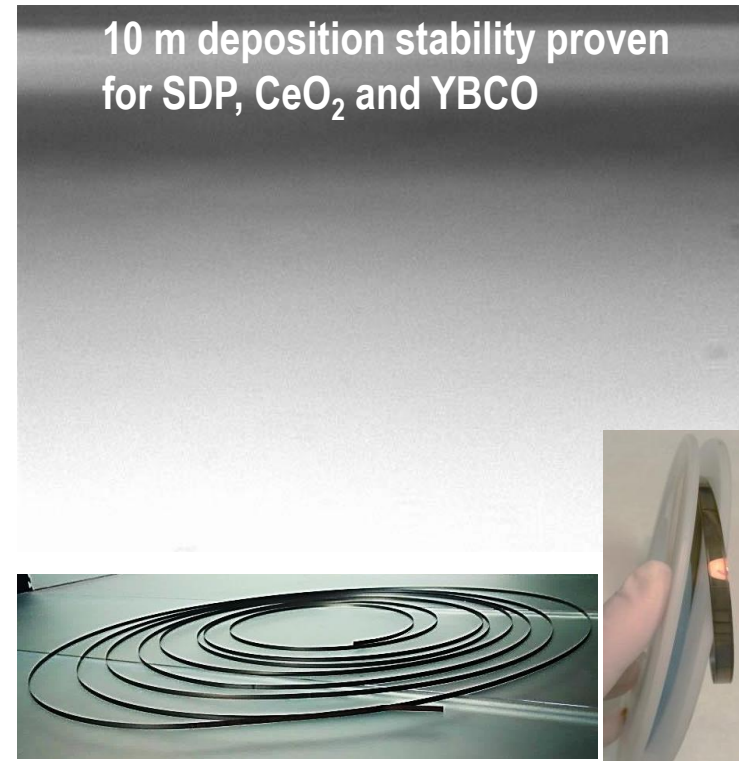
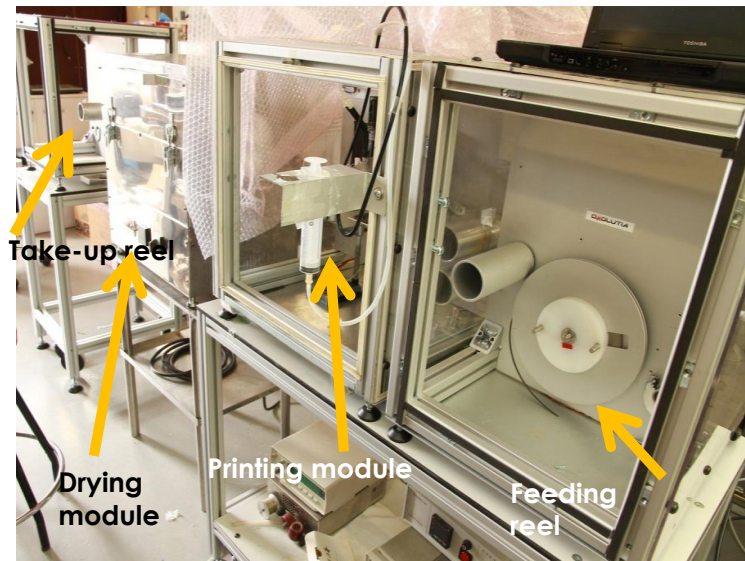


Expanded Pilot Line

T. Puig-EUCAS2015

Chemical Solution Deposition **OXOLUTIA** scalability processes at Oxolutia

Reel-to-reel Ink Jet Printing pilot plant for **all CSD** on
ABAD Bruker substrates

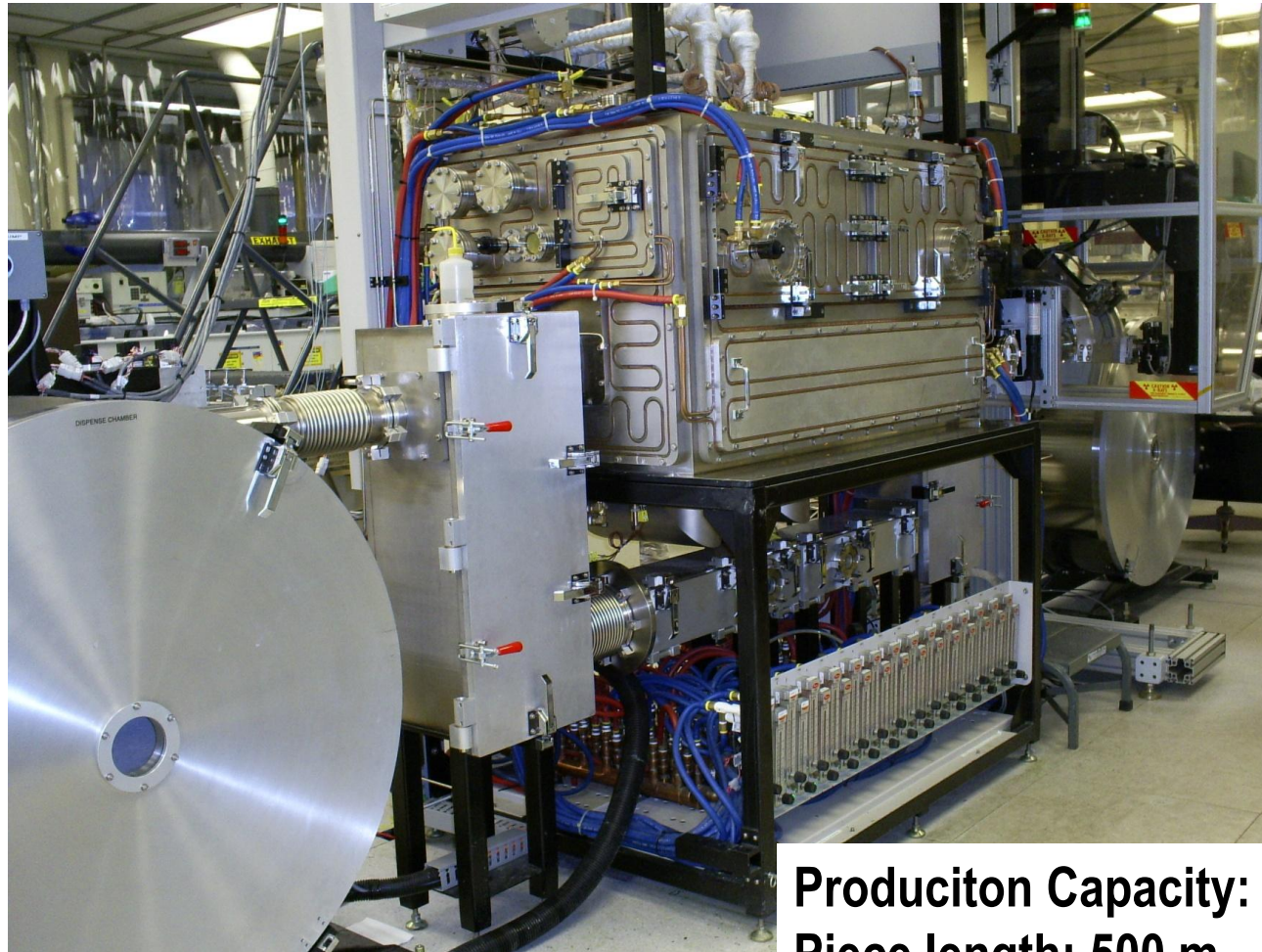


10 m CeO₂ buffer @ 28 m/h

1 m YBCO

T. Puig -EUCAS 2015

MOCVD approach on IBAD



Production Capacity: 1000 Km/yr
Piece length: 500 m

Installations at Fujikura



Installations at Showa

Batch furnace for TFA-CSD / IBAD



Production capacity : 20 Km/yr
Piece length: 125 m



T. Puig -EUCAS 2015



SuNAM (Korea): Production Facilities

RCE-DR on IBAD

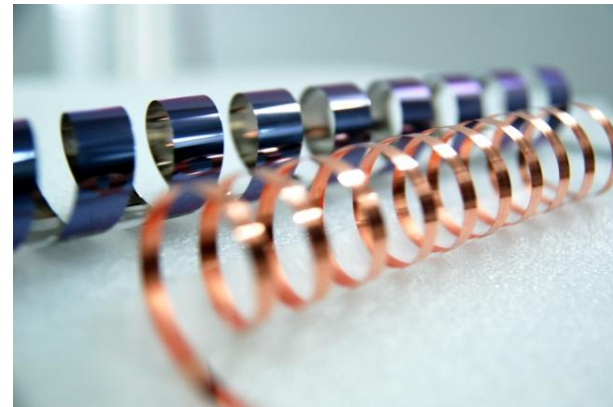
IBAD facility: ~17 m long



Production capacity: ~ 1000 km/yr. Piece length : 1 km



Reactive Co-Evaporation
Deposition and Reaction



T. Puig -EUCAS 2015



HTS at all magnetic fields

Cost/Performance

Figure of merit:
 €/kAm at specific T and H

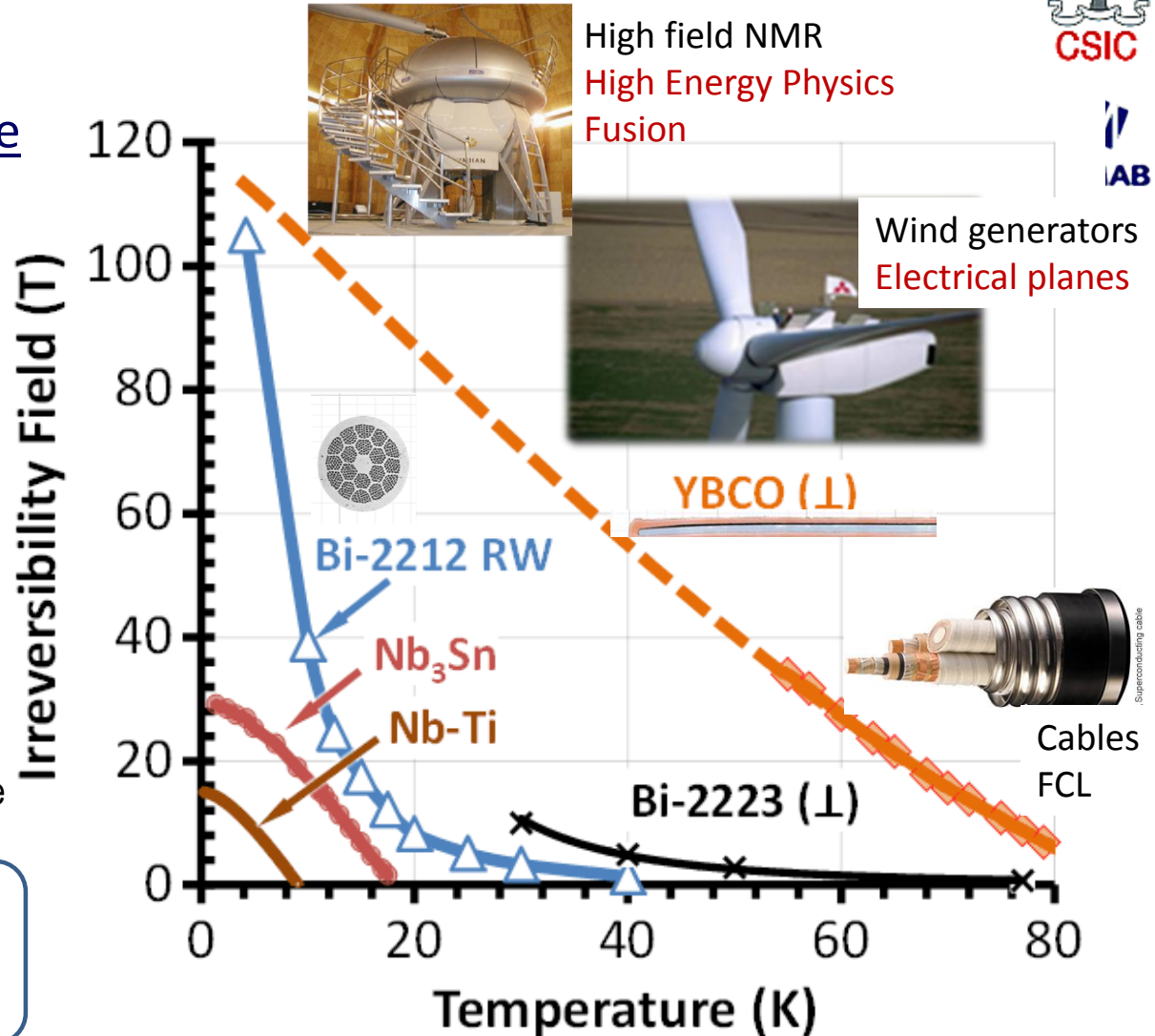
Present:

~200 €/kAm (77K, SF)
 ($I_c = 400$ A)

~100 €/kAm (30 K, 3T)
 ($I_c = 800$ A)

Further nano-structuration
 and production scalability
 expects a factor 4 decrease

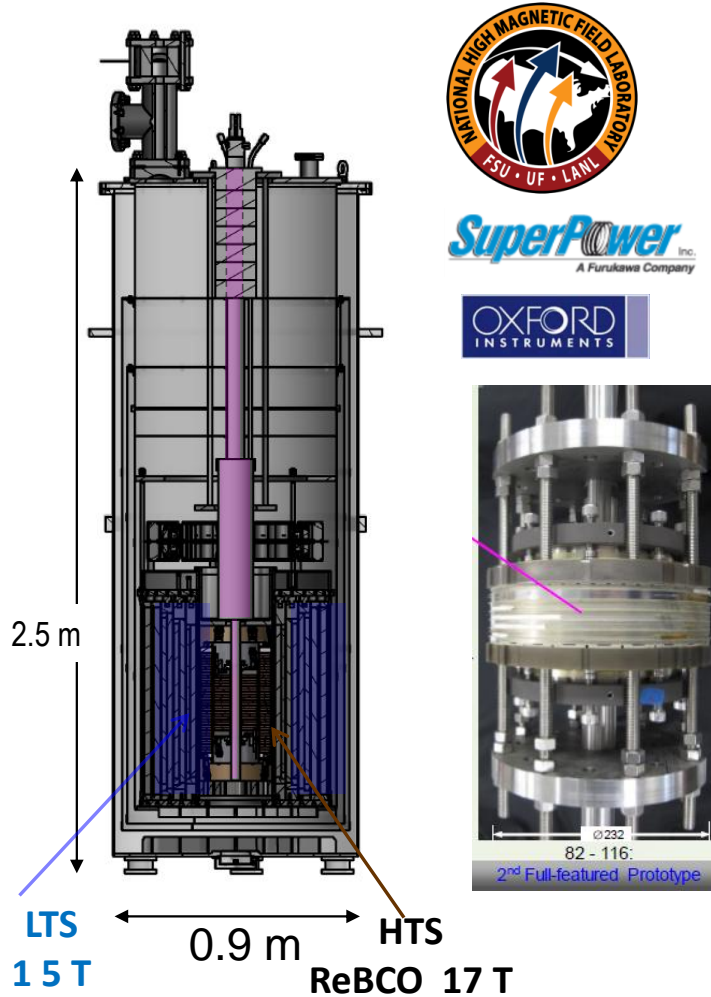
Estimated Market by
 2030: ~15.000 km/yr



D. Larbalestier, Nature Materials (2014)

T. Puig -EUCAS 2015

32 T LTS-HTS Magnet



26.4 T HTS Magnet

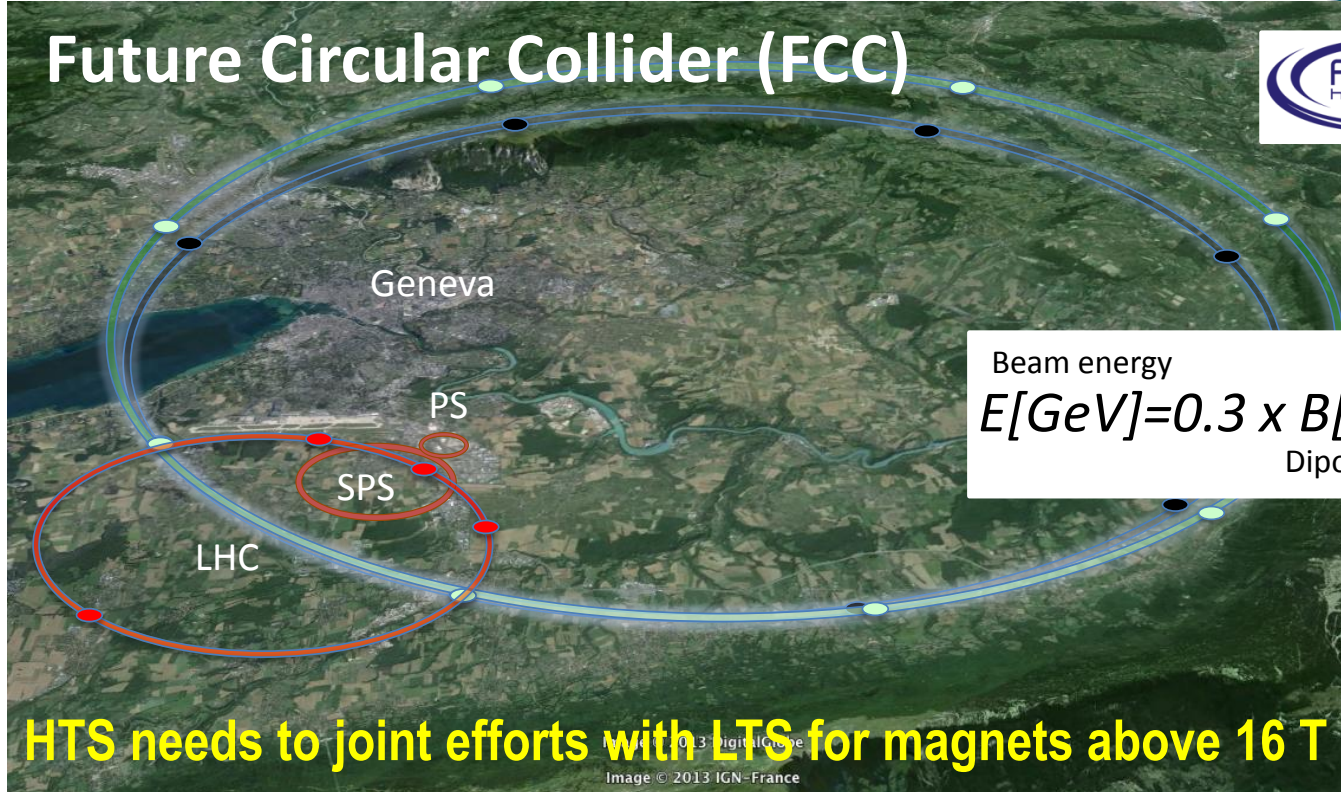
With Multi-Width and No-Insulation REBCO Wire



26 Double Pancake Coils Stacking

T. Puig -EUCAS 2015

The Call of High Energy Physics: LTS and HTS



LHC
 27 km, 8.33 T
 14 TeV (c.o.m.)
 1300 tons NbTi

Luca.Bottura@cern.ch

HE-LHC (2025)
 27 km, 20 T
 33 TeV (c.o.m.)
 3000 tons LTS
 700 tons HTS

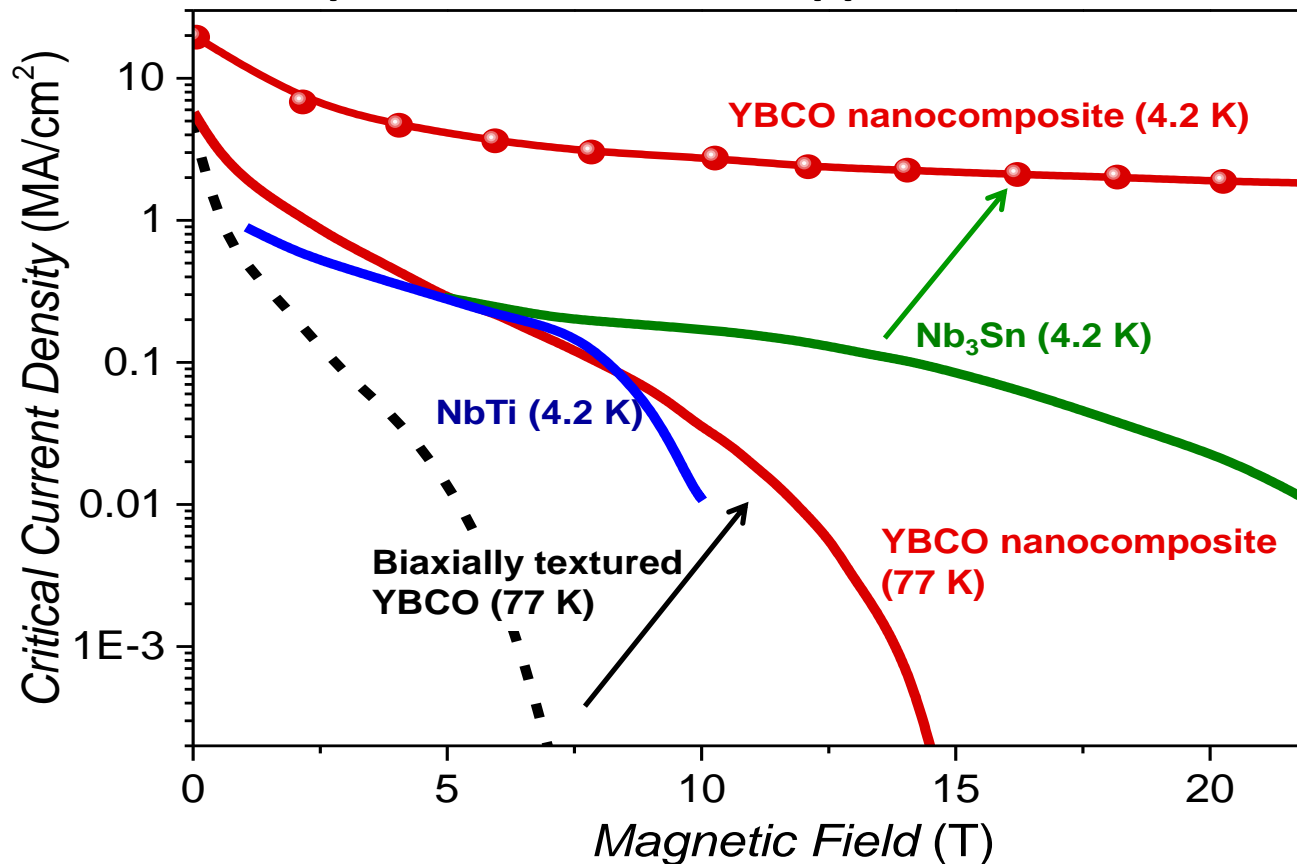
FCC-hh (2035)
 80 km, 20 T
 100 TeV (c.o.m.)
 9000 tons LTS
 2000 tons HTS

FCC-hh (2035)
 100 km, 16 T
 100 TeV (c.o.m.)
 6000 tons Nb₃Sn
 3000 tons Nb-Ti

T. Puig -EUCAS 2015

Nanotechnology engineering enables YBCO to improve at all regions

and postulate for low T applications

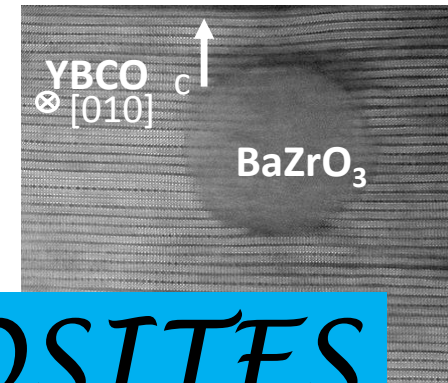
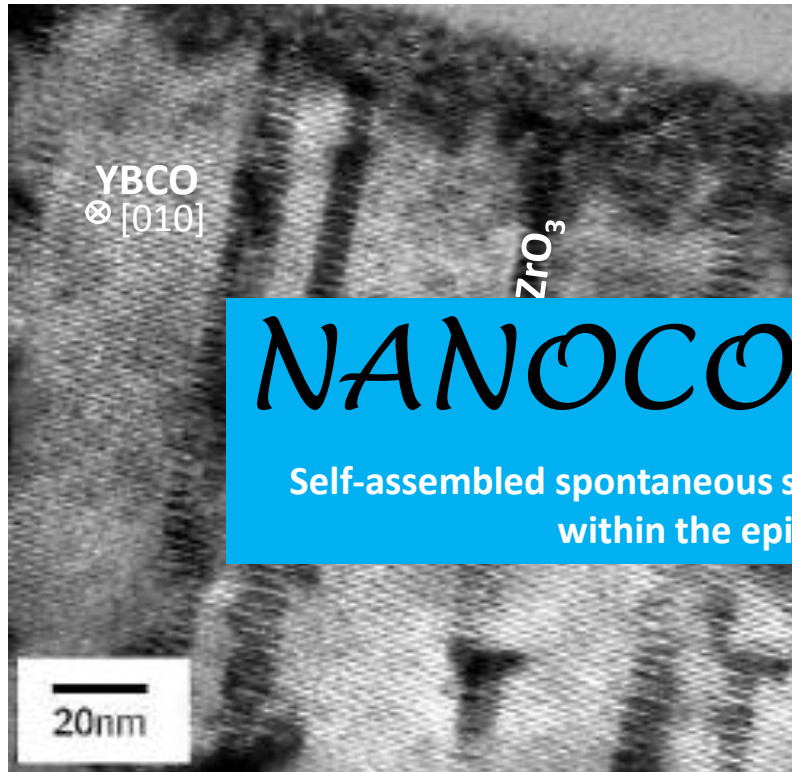


The outstanding push towards scalable Artificial Pinning Centers



By Pulsed Laser Deposition (also by MOCVD)

By Chemical Solution Deposition



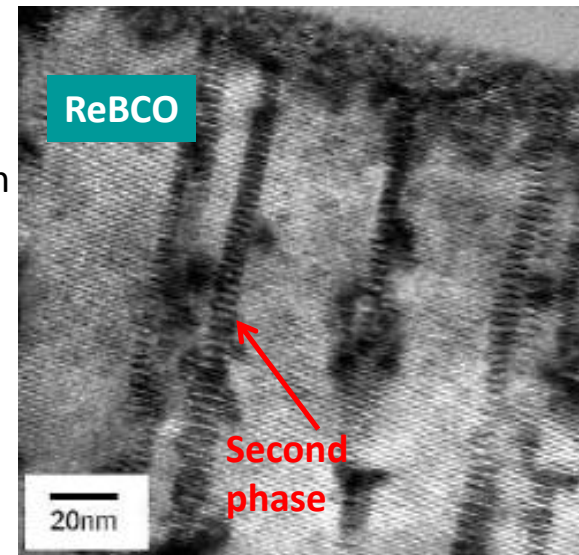
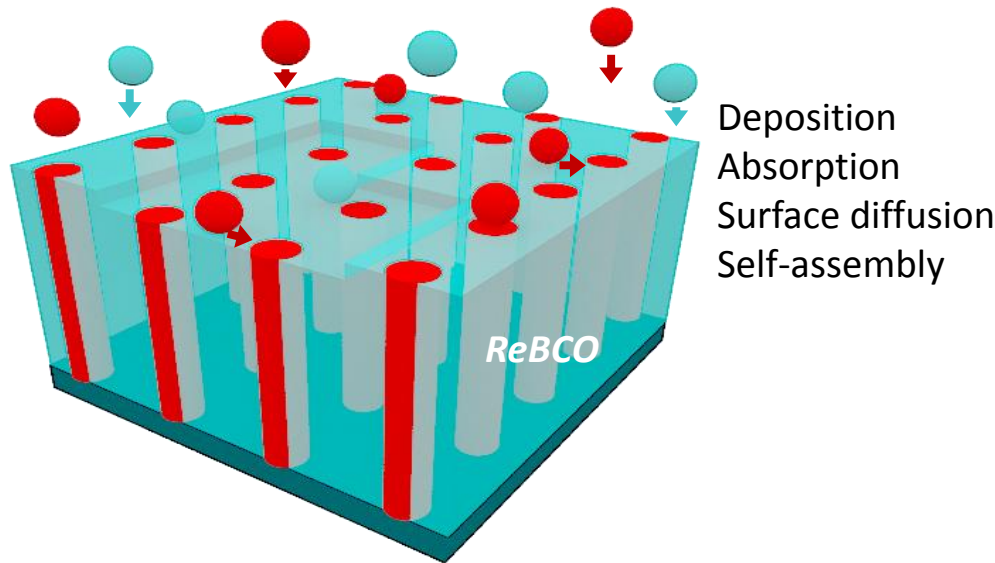
NANOCOMPOSITES

Self-assembled spontaneous segregation of second nano-phases
within the epitaxial YBCO matrix

- J. Driscoll, Nat. Mat. 3(2004); J. Haugan, Nature 430(2004)*
Y. Yamada, APL 87(2005); S. Kang, Science 311 (2006)
B. Maiorov, Nat Mat 8 (2009); A Kiessling, SUST 24 (2011)
J. Guiterrez, Nat Mat 11 (2007)
A. Llordés, Nat Mat 6 (2012)
M. Miura, SUST 26 (2013), M. Miura, SUST 23(2010)
S. Engel, APL 90 (2007)
T. Puig -EUCAS 2015

Growth of ReBCO Nanocomposites

Simultaneous deposition and growth (Case PLD, MOCVD and HLPE)



- Epitaxial nanorods form with YBCO simultaneously
- Semicoherent interfaces between nanorods and YBCO induce localized strain

Pulsed Laser Deposition (PLD): **Physical vapor deposition**

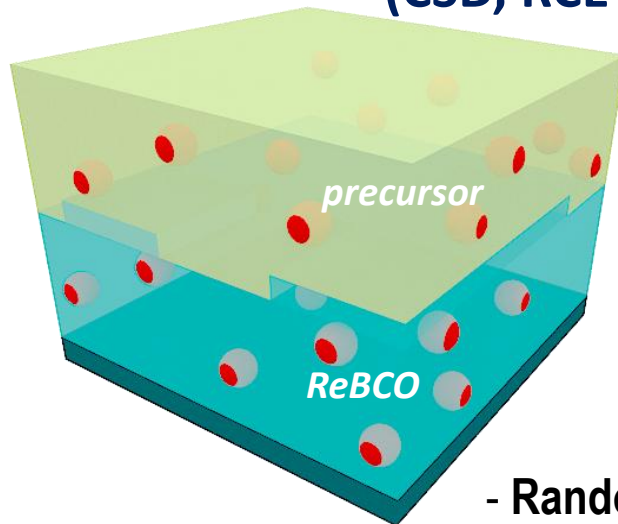
Metalorganic chemical vapor deposition (MOCVD): **Chemical vapor deposition**

Hybrid liquid phase epitaxy (HLPE): **Physical deposition with solid-liquid reaction**

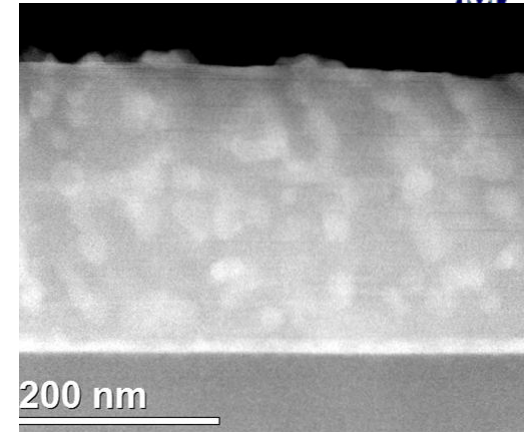


Growth of ReBCO Nanocomposites

Sequential deposition and growth (CSD, RCE-DR and CSD-TLAG cases)



Precursor deposition
Nanoparticles formation
ReBCO conversion and
trapping of nanoparticles



- Random oriented nanoparticles form prior to YBCO
- A heavily long range isotropic nanostrained matrix

Chemical Solution Deposition of metalorganics (MOD-CSD)

Chemical gas-solid conversion

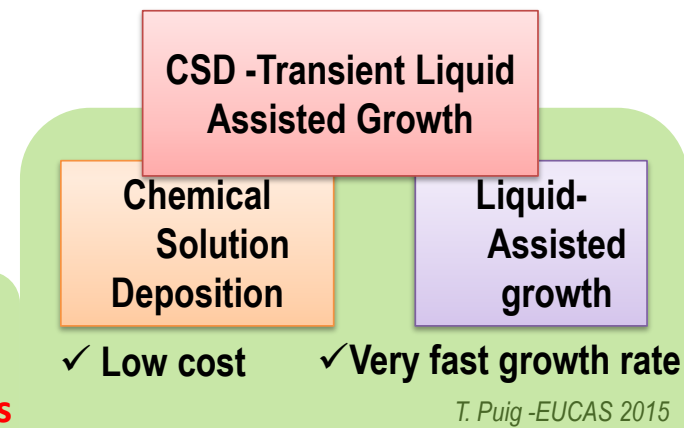
Reactive co-evaporation by deposition and reaction (RCE-DR)

Physical co-evaporation and fast conversion from a liquid



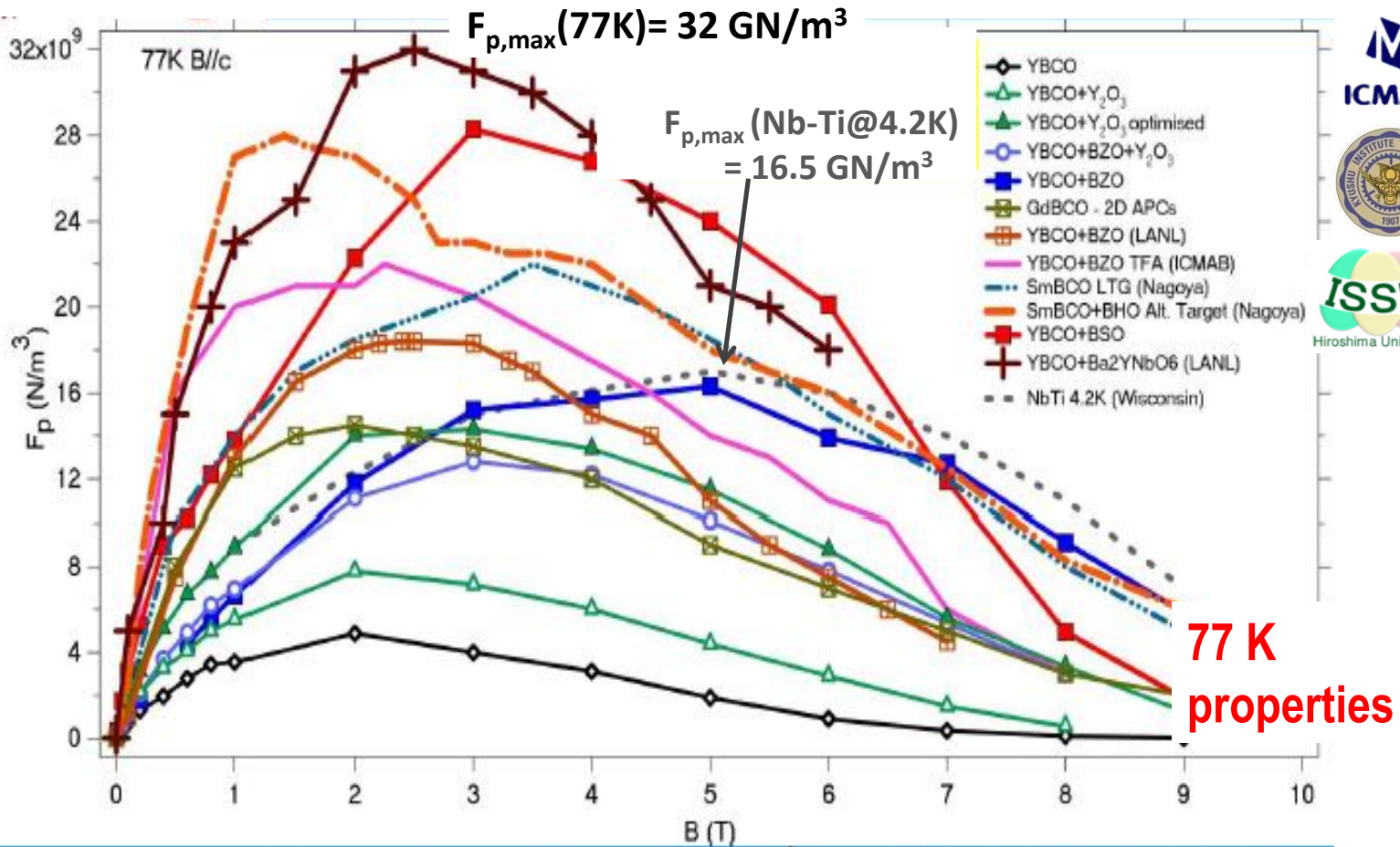
**CSD- Transient Liquid Assisted Growth
(CSD-TLAG)**

Fast liquid-solid reaction from CSD precursors



T. Puig -EUCAS 2015

Strong increase of Pinning Force ($F_p = J_c \times B$) by Nanocomposites

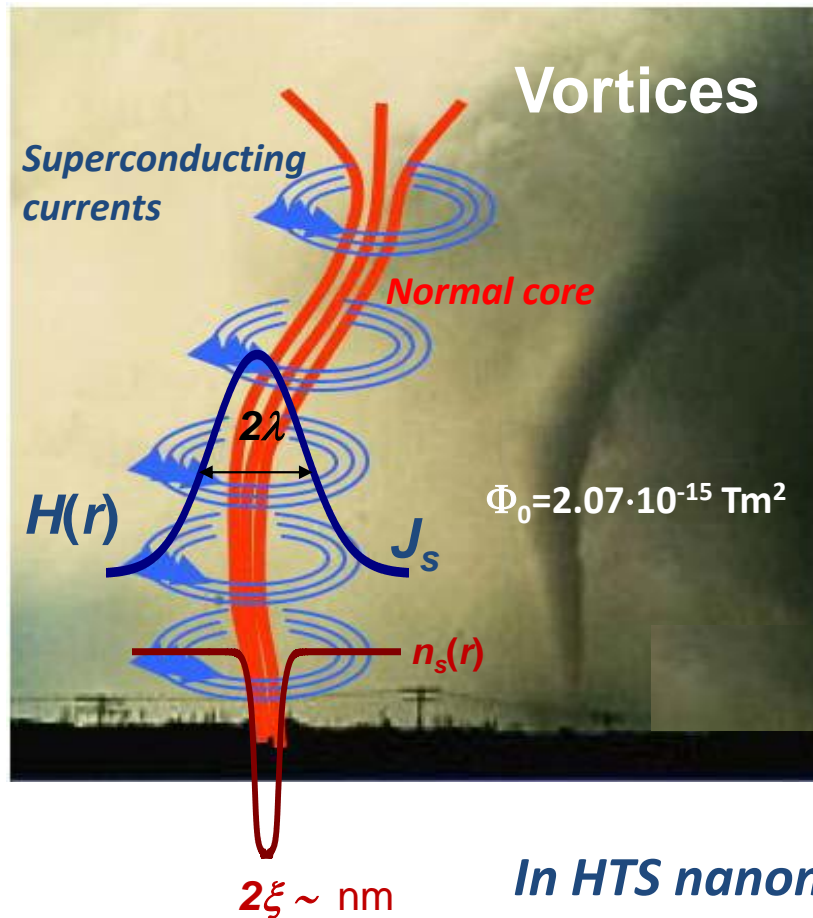


X.Obradors, T. Puig, A. Palau, F. Sandiumenge, P. Mele, K. Matsumoto – “Nanostructured Superconductors with efficient vortex pinning” in Comprehensive nanoscience and nanotechnology, AP, Vol 3 (2011) 303-349 [added with YBCO+Ba2YNbO6 and SmBCO+BHO]

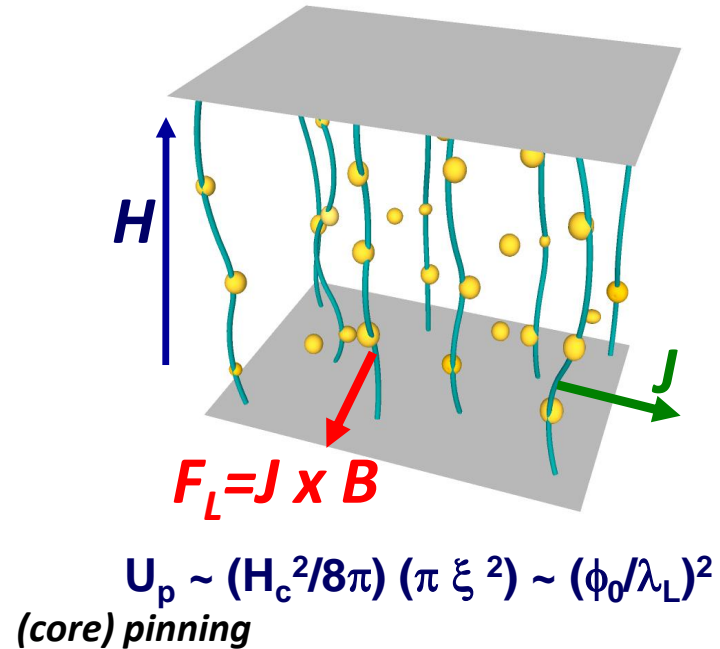
T. Puig -EUCAS 2015



It is all about Vortices ... quantized flux lines



Their motion and the role of pinning centers



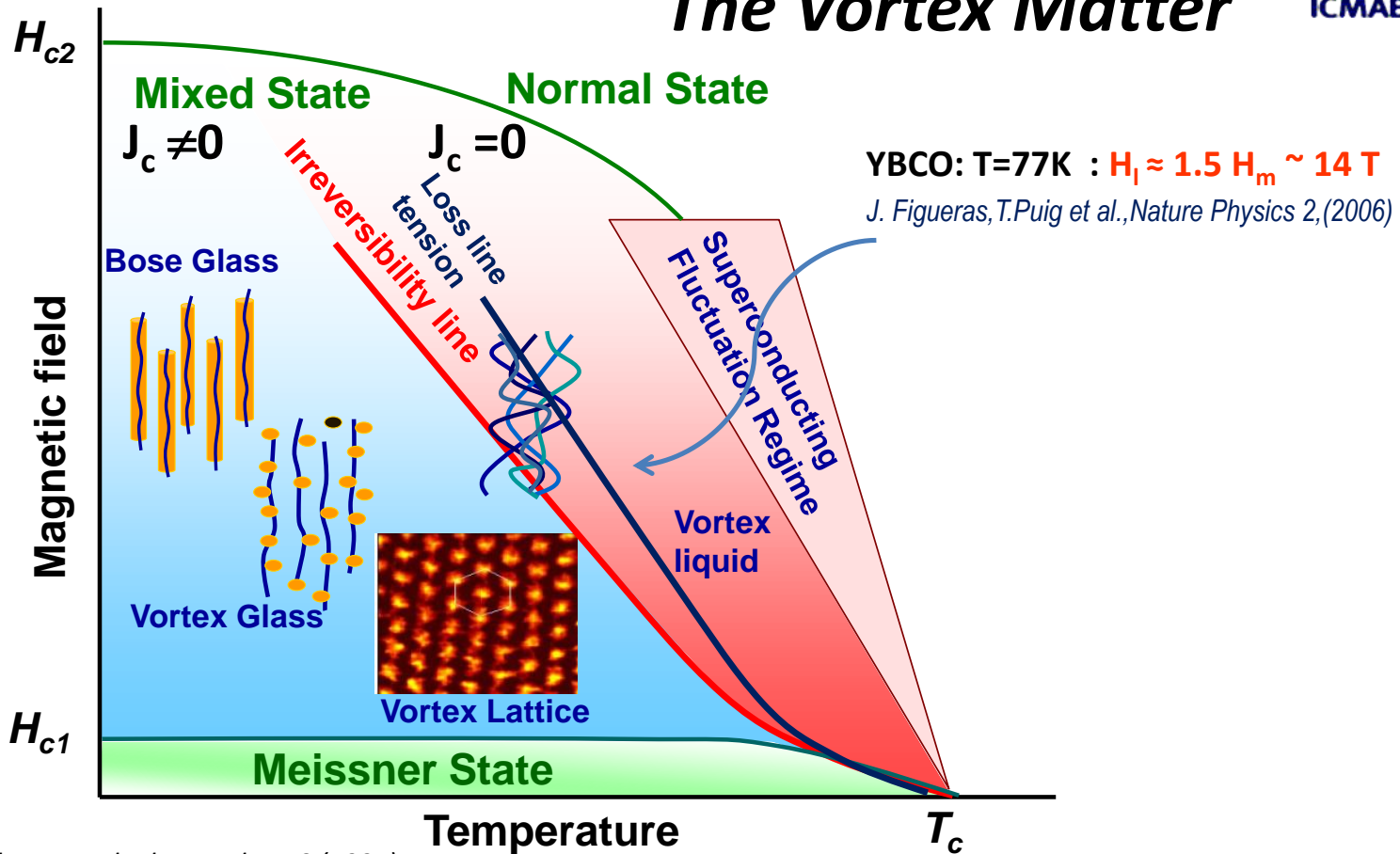
In HTS nanometer defects get into the game



Abrikosov Vortices in HTS

Thermal fluctuations, elastic energy, pinning energy and vortex-vortex repulsion play relevant roles

The Vortex Matter



G.W. Crabtree et al, Phys. Today 50 (1997)

T. Puig -EUCAS 2015

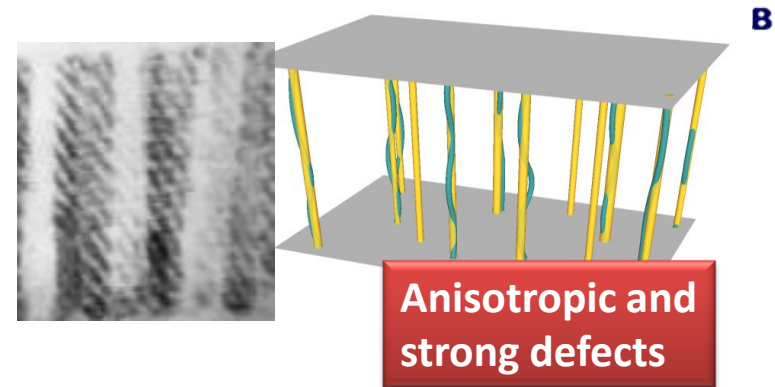
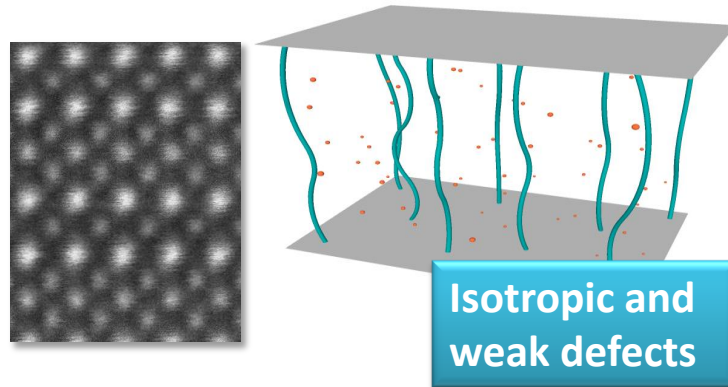


Vortex Pinning Centers in HTS

Great variety of pinning sites and complex vortex matter

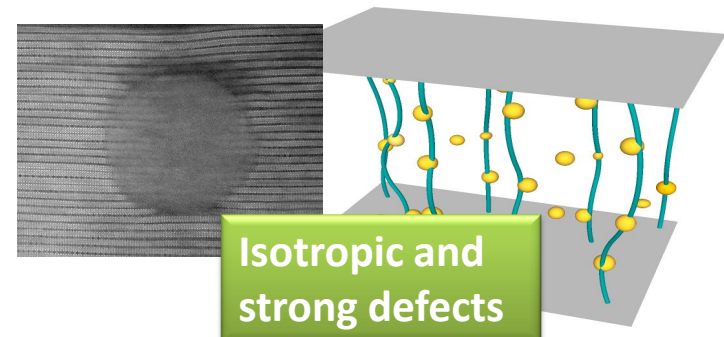
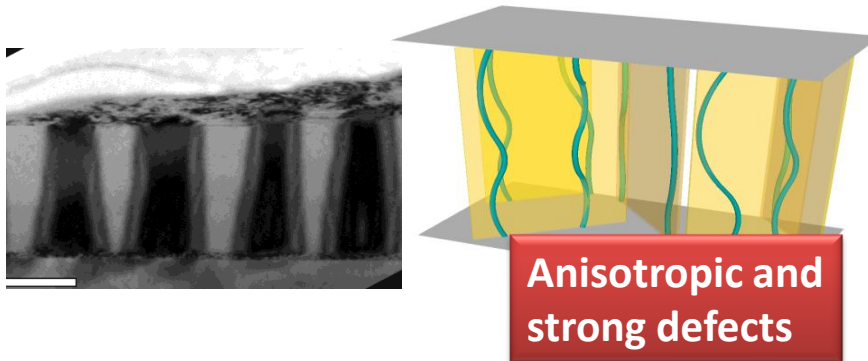
0D-PC: Oxygen vacancies, element substitutions, **point defects**

1D-PC: Dislocations, **columnar defects**



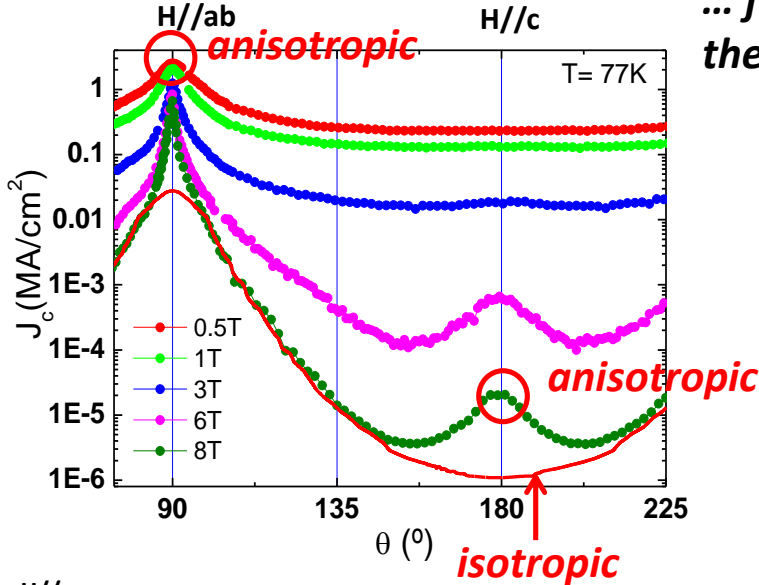
2D-PC: Grain boundaries, **twin boundaries**, planar defects

3D-PC: **Precipitates**, secondary phases, local strain

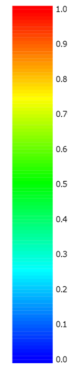
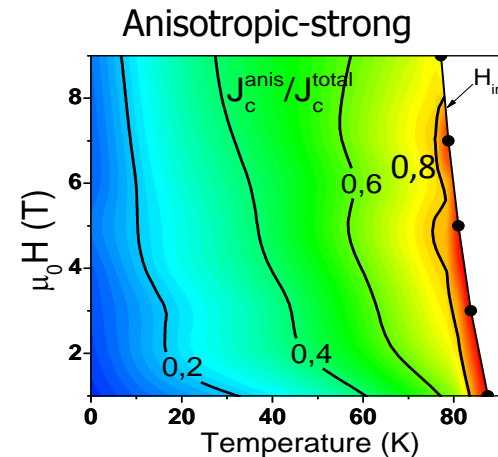
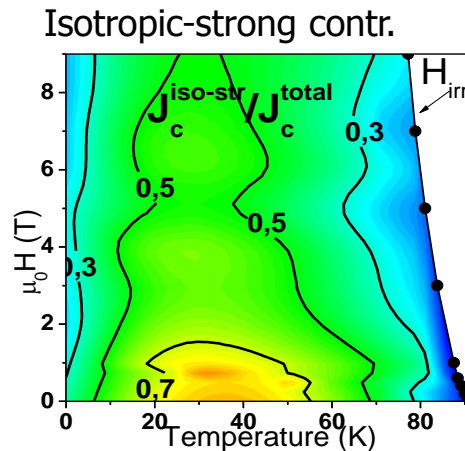
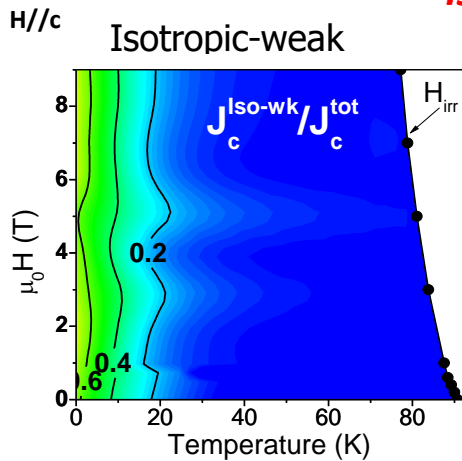
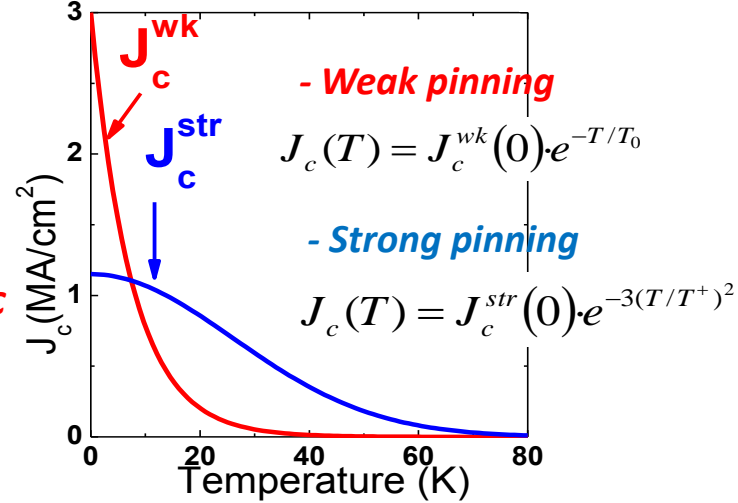
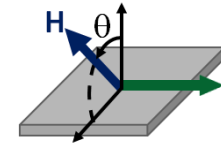


Nanoengineering is the path towards control of vortex pinning and enhance performances. Interaction with natural defects to be considered *T. Puig -EUCAS 2015*

Pinning strength diagrams



... from $J_c(H, T, \theta)$ we separate the different components



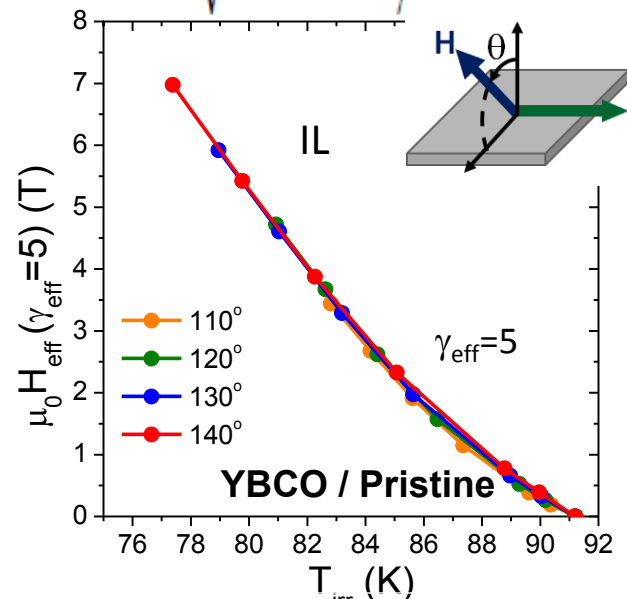
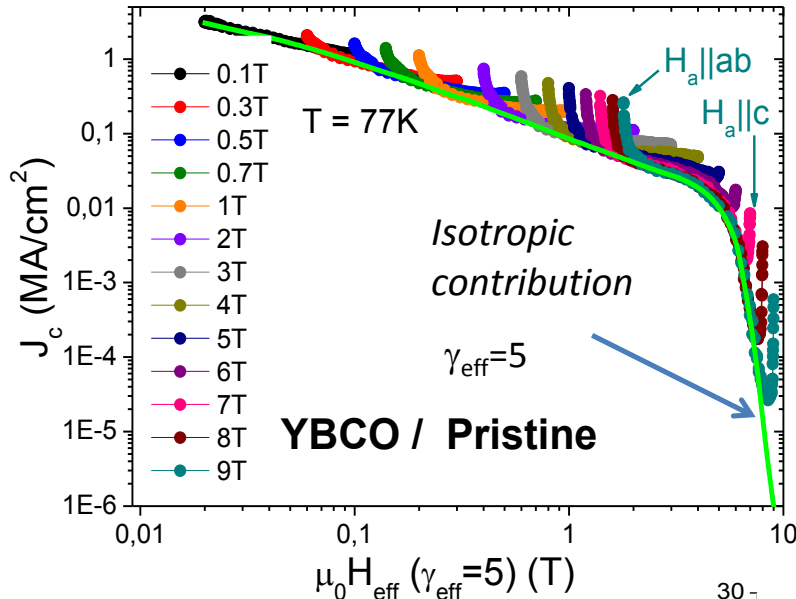
T.Puig et al., SUST 21, 034008 (2008); J. Plain et al., PRB 65, 104526 (2002); J.Gutierrez et al., Appl. Phys. Lett. 90 (2007)

T. Puig -EUCAS 2015

Anisotropy of Critical Currents, I_L and H_{c2}

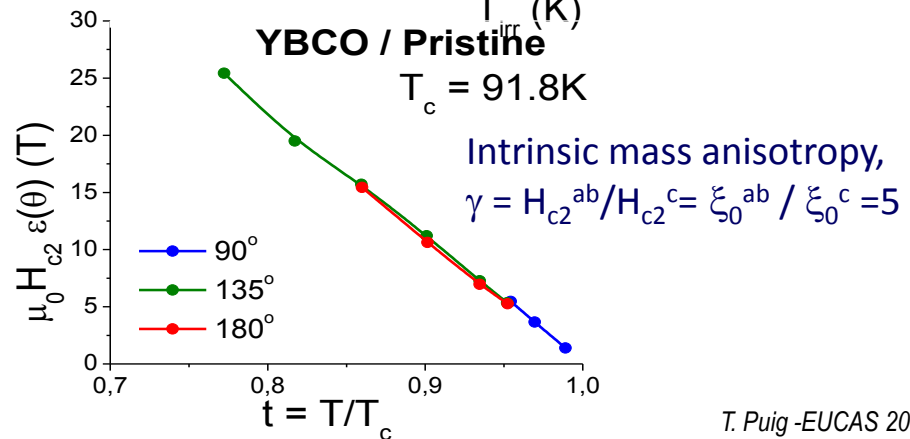


Blatter scaling approach $H_{eff} = H_a \varepsilon(\theta) = H_a \sqrt{\cos^2 \theta + \frac{1}{\gamma^2} \sin^2 \theta}$



Pinning Anisotropy (J_c, I_L) = γ_{eff}

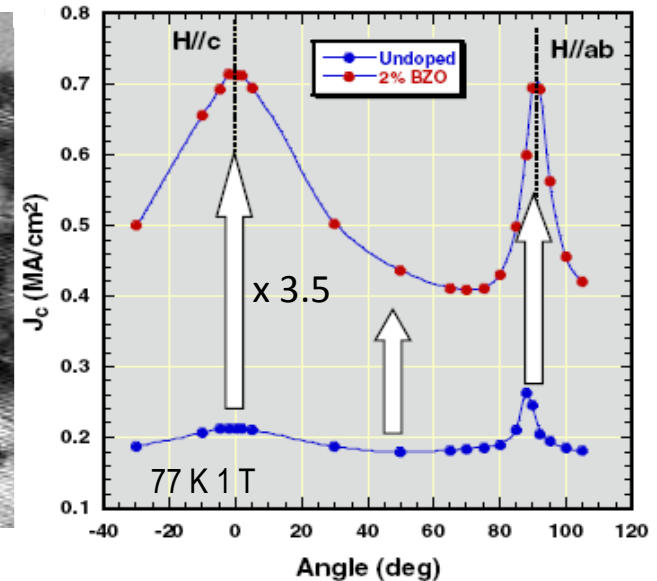
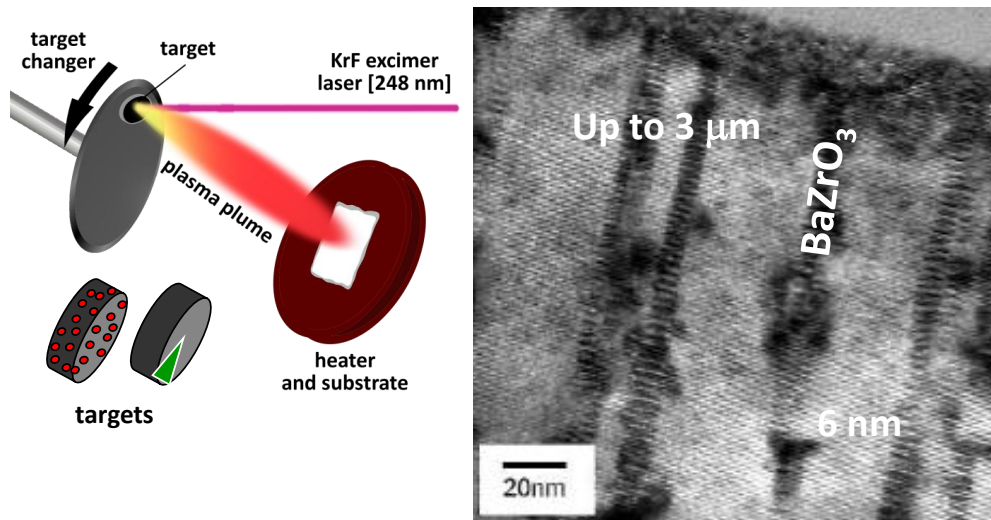
$\gamma_{eff} = \gamma$ in YBCO films and most nanocomposites
 $\gamma_{eff} < \gamma$ specially in CSD nanocomposites





The Breakthroughs of Nanocomposites by PLD

A physical vapor phase growth method giving rise to a self-assembly process of nanocolumns through spontaneous phase segregation



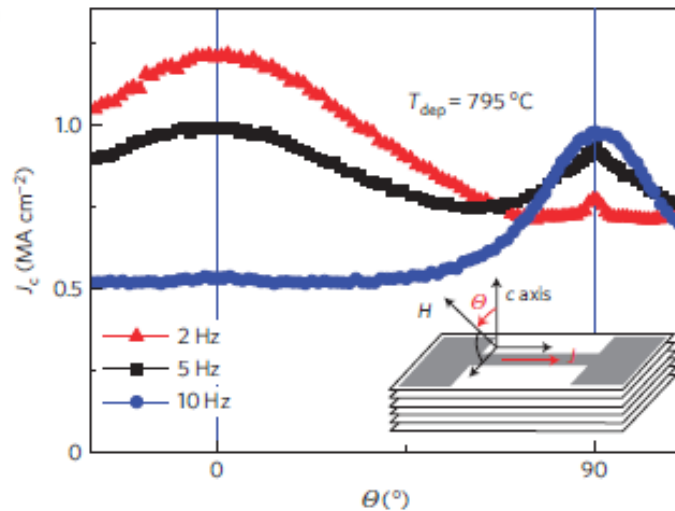
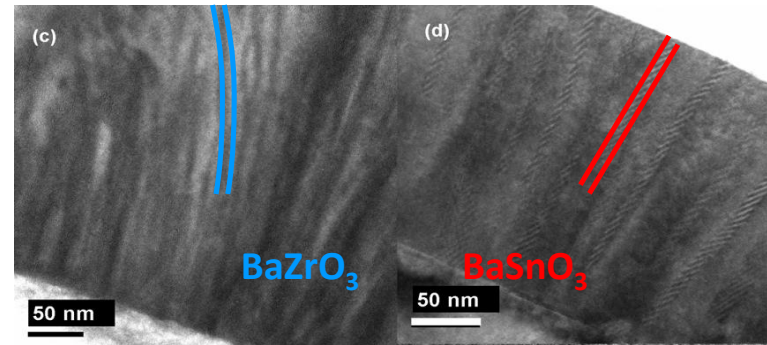
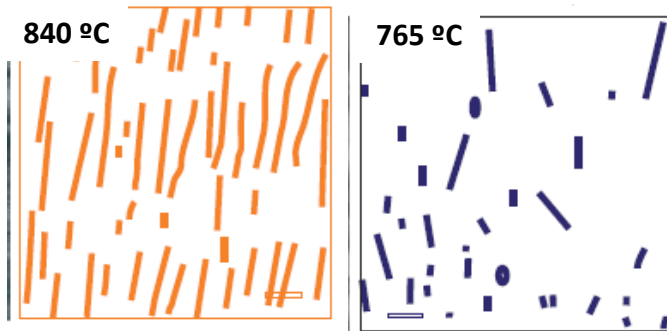
First demonstration of 3D epitaxial self-assembly in complex functional oxides

Anisotropic increase of performance with BaZrO₃ nanorods

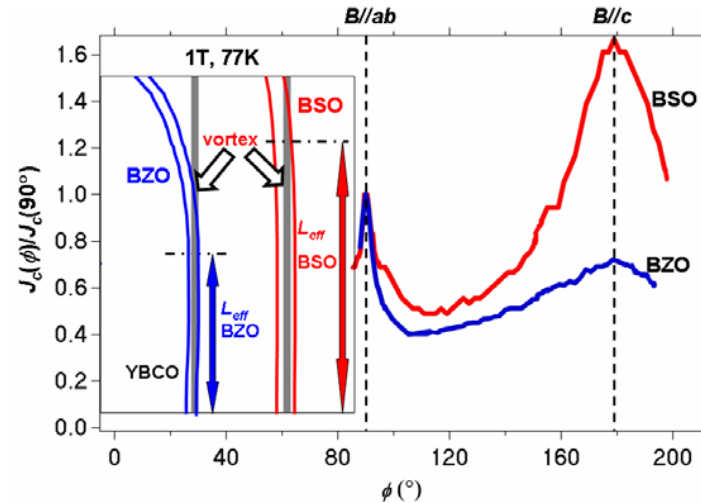
Anisotropic (correlated) pinning

Tunability of Nanocomposites by PLD

Growth temperature, growth rate, second phase composition determine self-assembling with direct consequences on J_c



Maierov et al. Nature Mat. 8(2009)

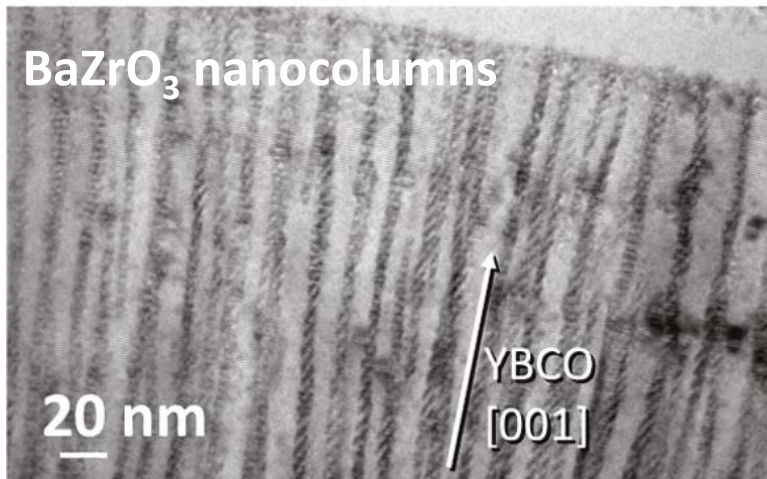


P. Mele et al, Supercond. Sci. Technol. 21 (2008)

T. Puig -EUCAS 2015

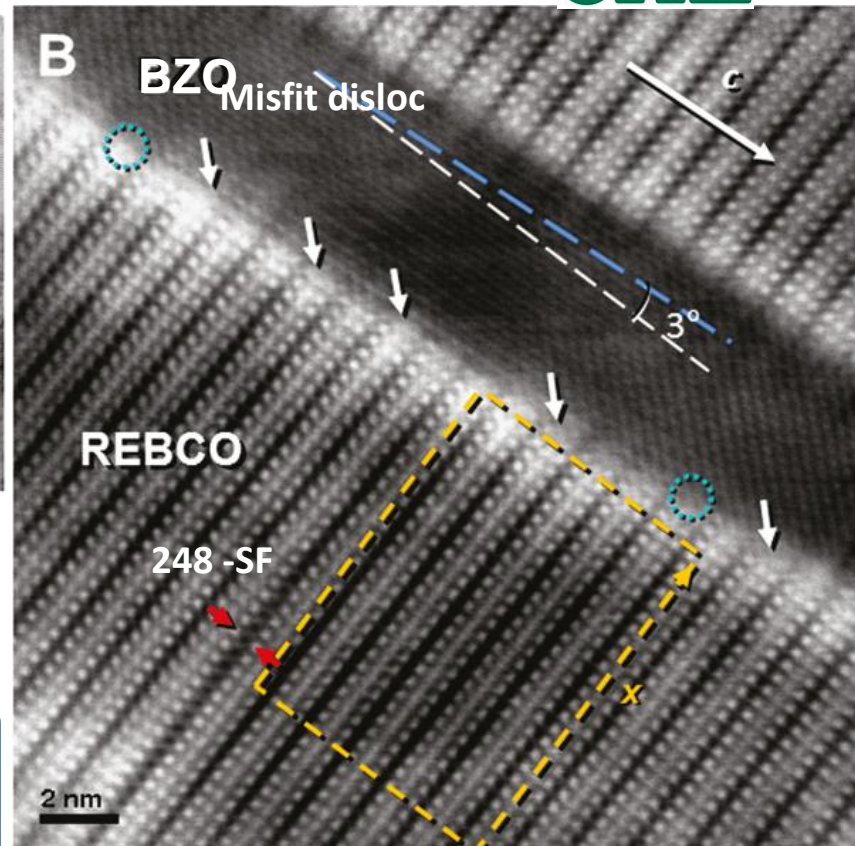
Self-assembly in PLD Nanocomposites

Strain field develop around the nanocolumns to reduce boundary energy inducing self-assembly



Misfit dislocations form at the YBCO/ BZO interface giving rise to a semicoherent strained boundary

Nanocolumns are pinning centers, but associated strain may also induce isotropic pinning at low T



C. Cantoni et al, ACSNano 2011

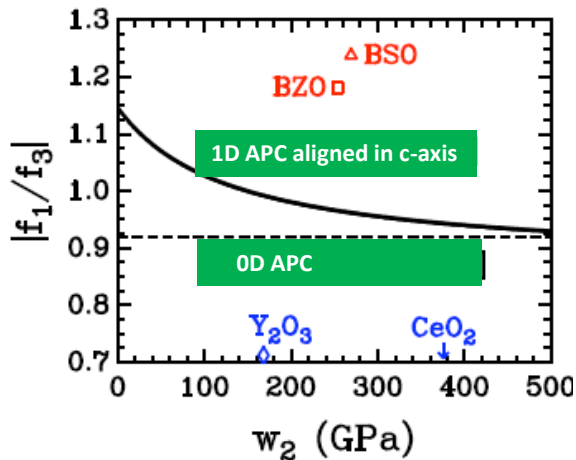
T. Puig -EUCAS 2015



Elastic Strain Model

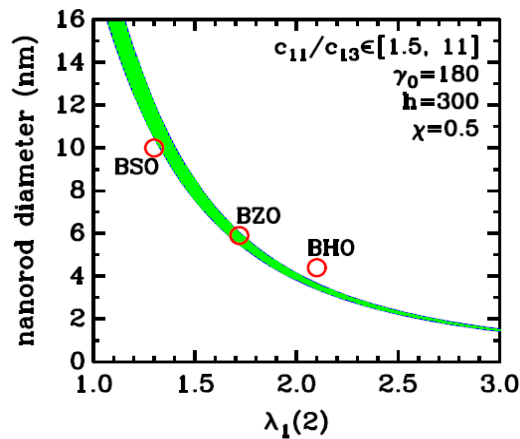
Understanding & controlling self-assembly of Artificial Pinning Centers

Dimensionality of APC
 depend on elastic properties
 and lattice constants



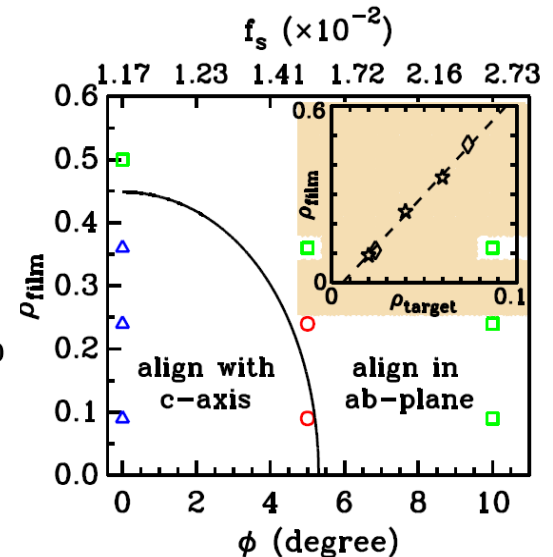
J. Shi and J.Z. Wu, *Philosophic Magazine* 92, 2911 (2012); 92, 4205 (2012).

Nanorod diameter
 depends on the inverse
 strain decay length $\lambda_1(2)$



J. Wu, et al, *SUST* 27, (2014);
 Shi and Wu, submitted

APC alignment direction
 depends on APC
 concentration and strain



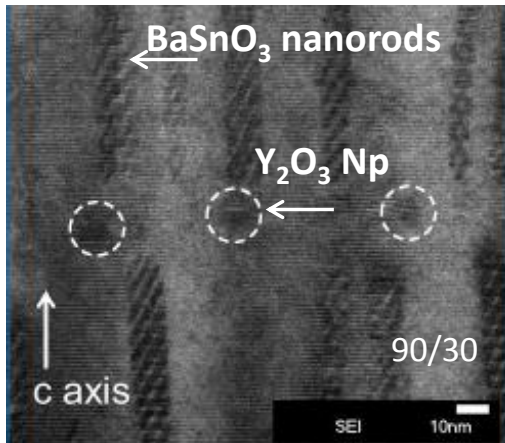
F.J. Baca, et al, *Advanced Functional Materials* 23, (2013); J. Wu, et al, *IEEE TAS* 25 (2015); Wu et al, submitted

Advanced APC structures by PLD

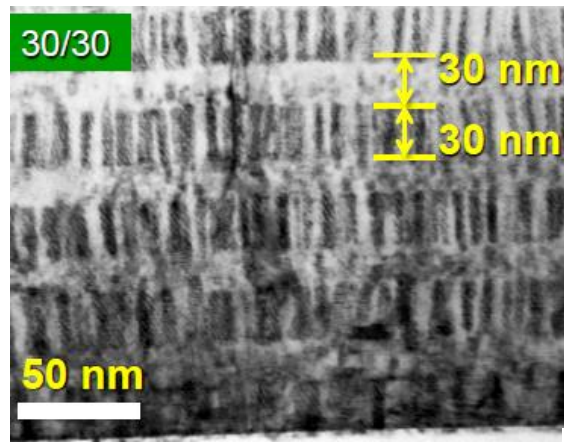
Opportunities to tune Isotropic / anisotropic performances



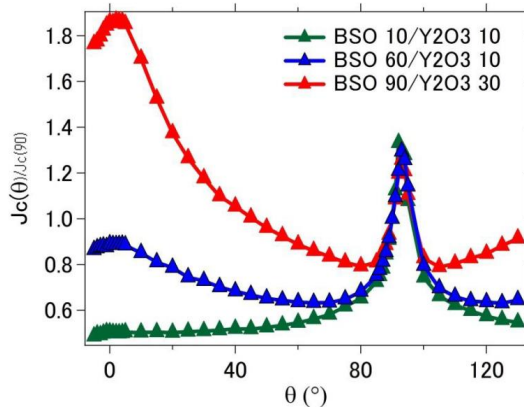
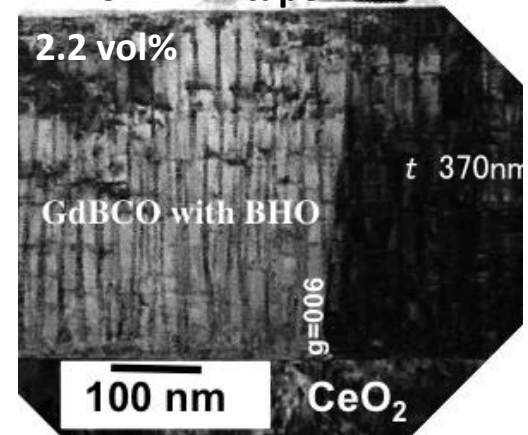
Hybrid multilayers



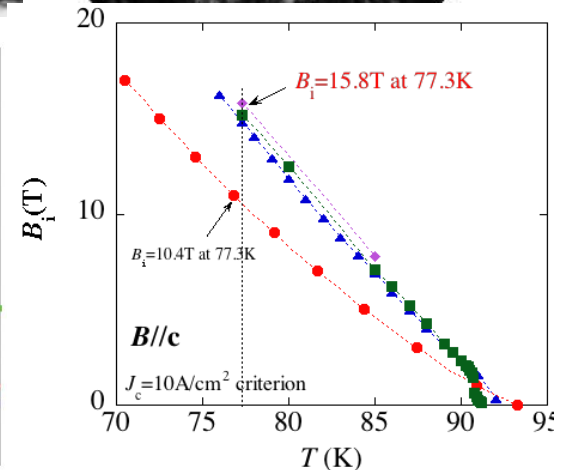
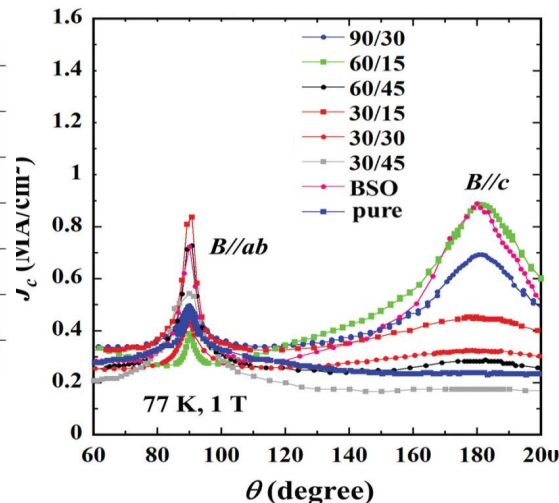
Segmented BaSnO₃ nanorods



GdBa₂Cu₃O₇-BaHfO₃ on IBAD tape

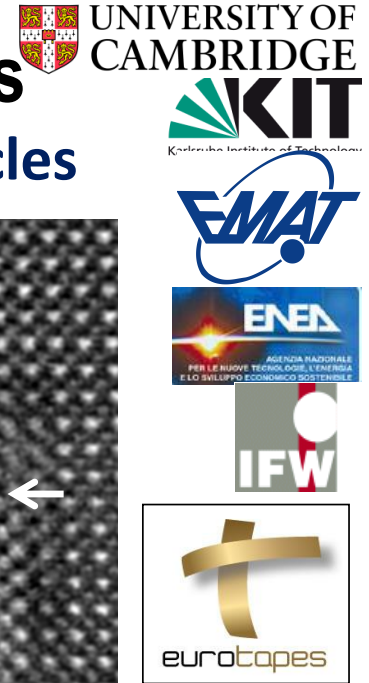


K. Matsumoto et al, 116 (2014)



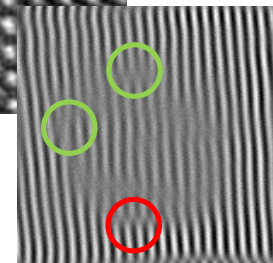
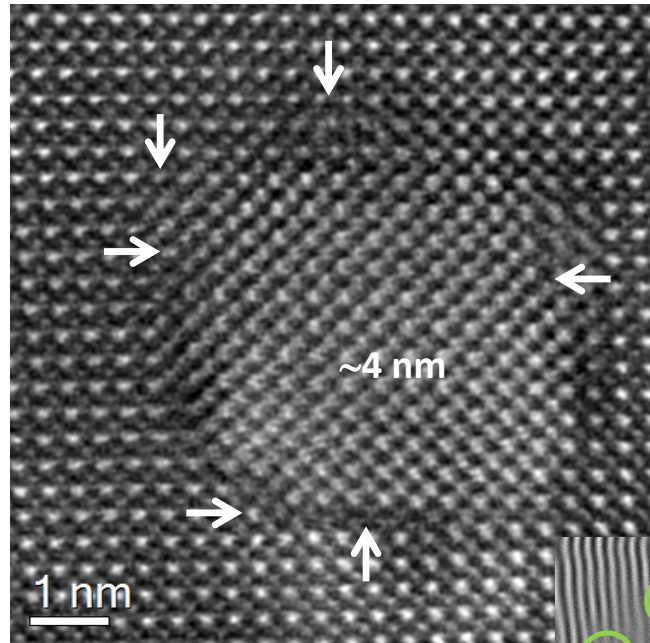
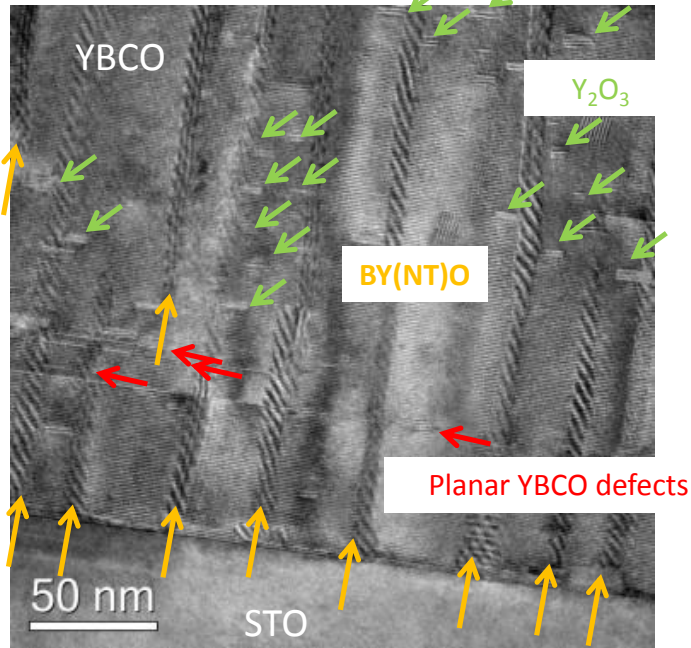
S. Awaji et al, APEX 8 (2015)

T. Puig -EUCAS 2015

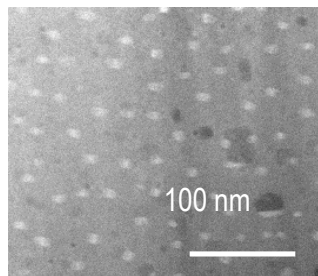


Mixed double perovskite nanocomposites

$Ba_2Y(Nb_{0.5}Ta_{0.5})O_6$ nanorods and Y_2O_3 nanoparticles



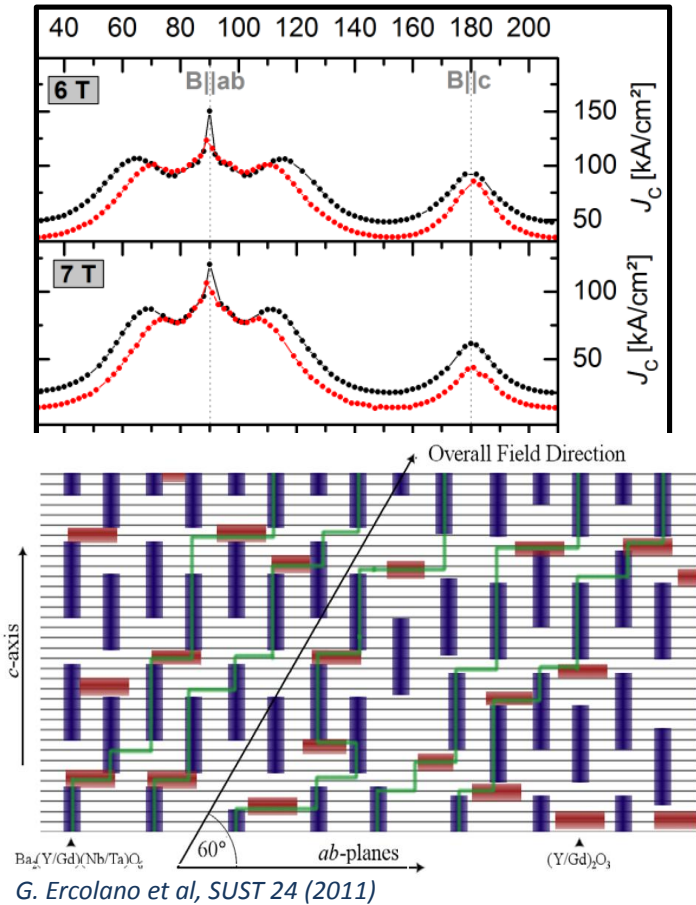
10% cell parameter difference between YBCO and BYNTO causes the presence of misfit dislocations



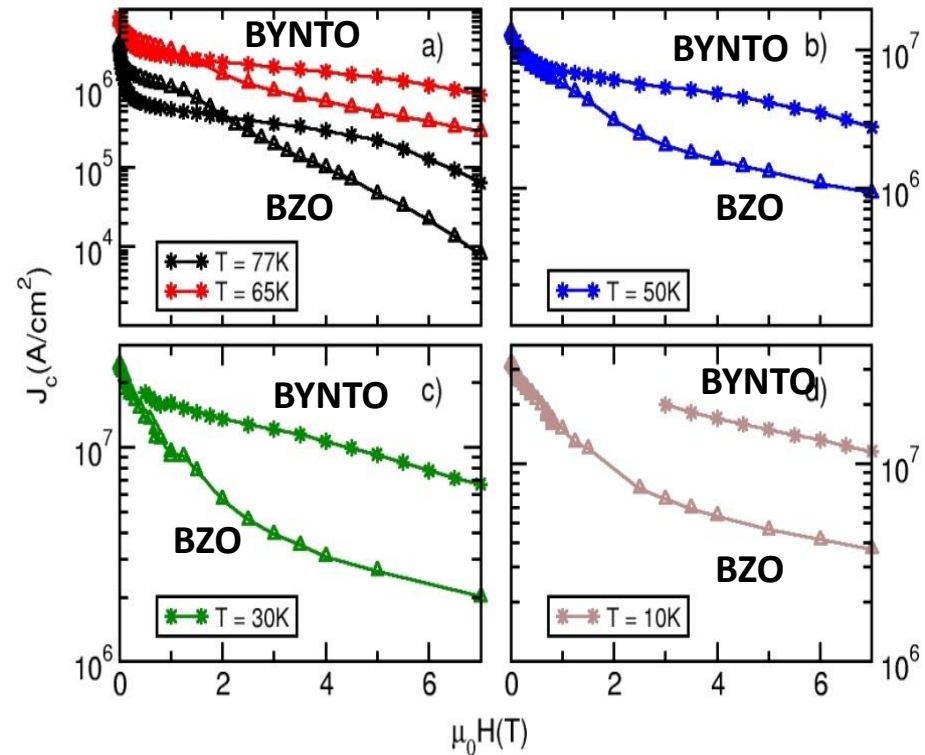
1 column / 30 nm
 $\rightarrow B_m = 2.2 T$

Rich pinning landscape \rightarrow Complex J_c dependencies expected

High pinning properties by mixed double perovskites



Vortices accommodate simultaneously to nanorod-segments and nanoplatelets

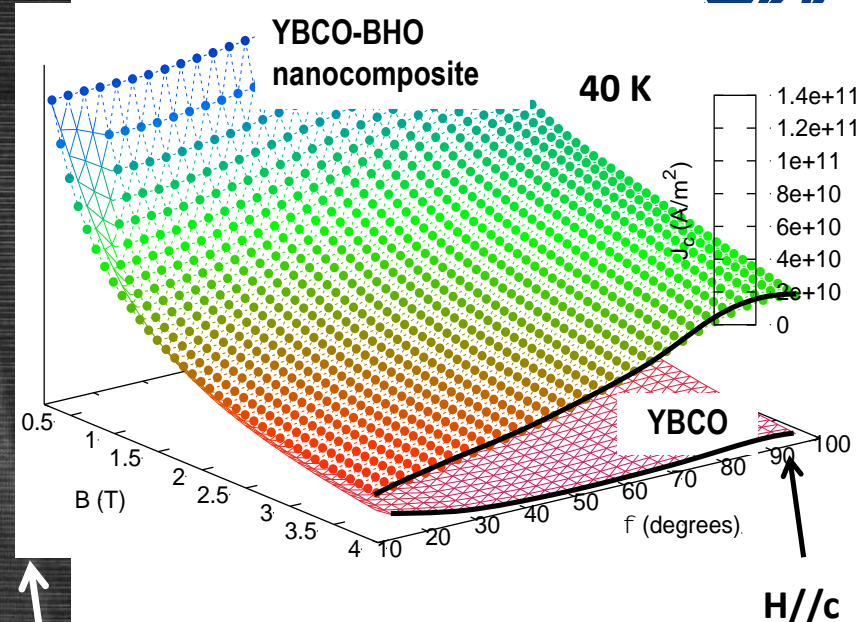
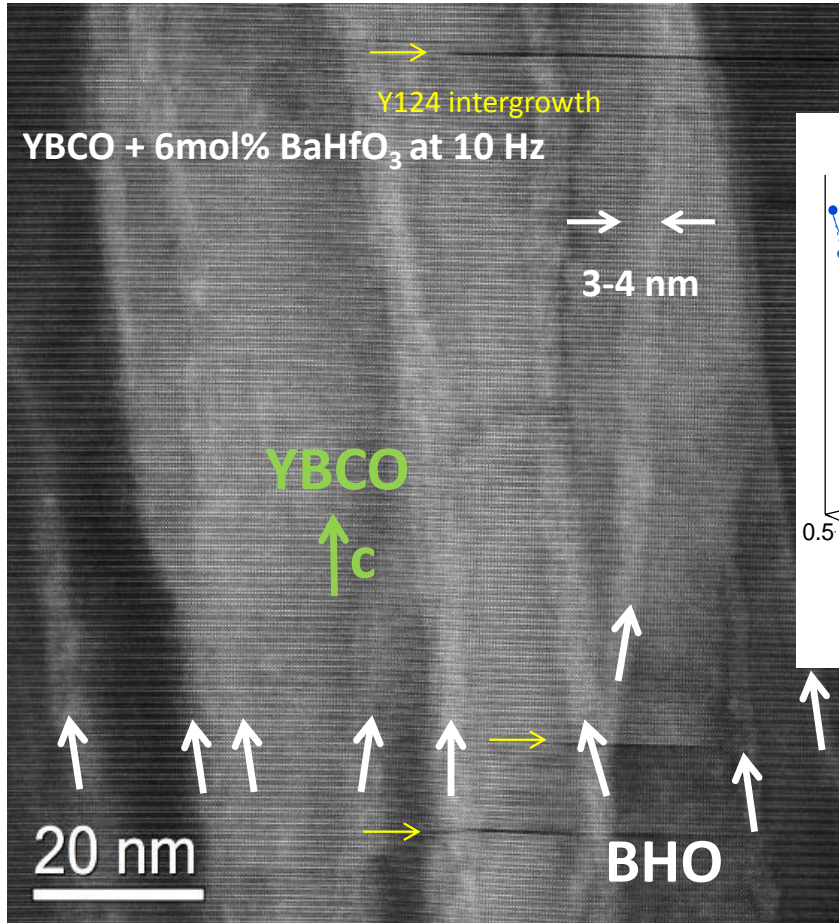


$F_{pmax} = 25 \text{ GN/m}^3$ at 77 K
 $F_{pmax} = 750 \text{ GN/m}^3$ at 10 K

among the highest values in literature

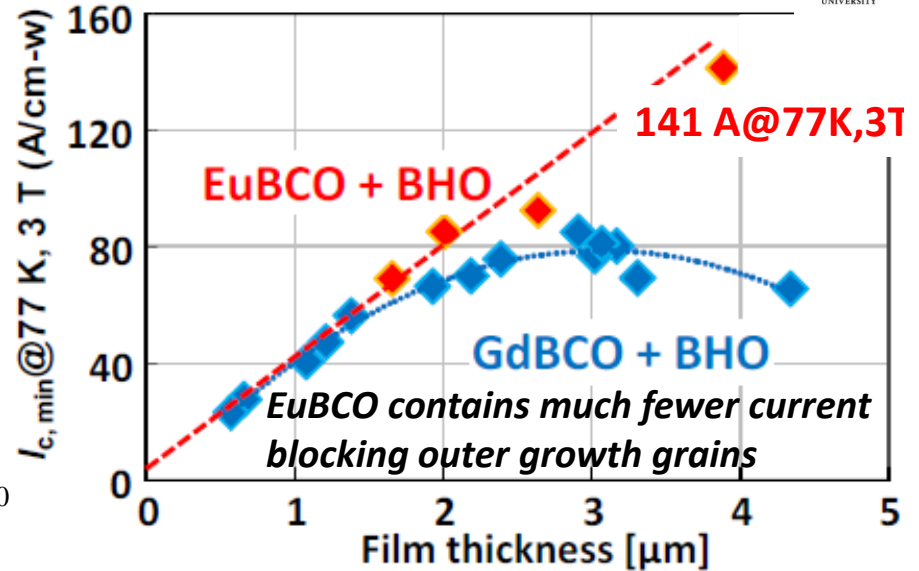
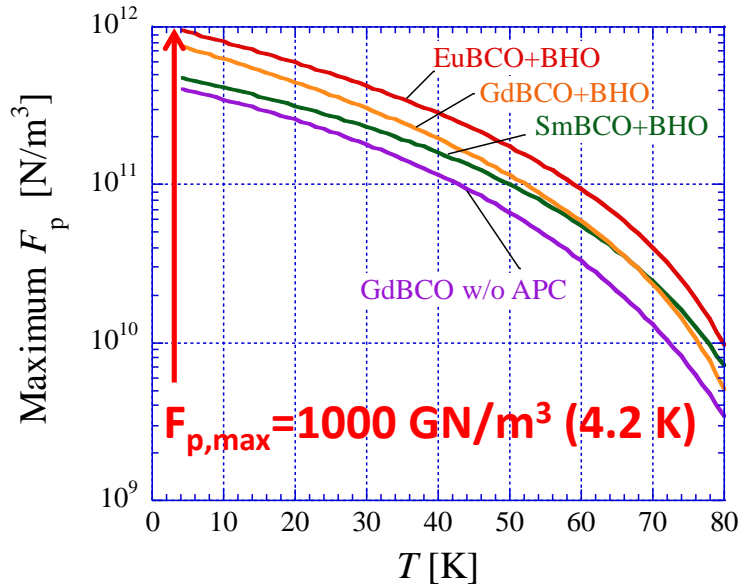
Fan-shaped BaHfO₃ nanorods by High Rate PLD on YSZ^{ABAD} substrates

Laser Frequency = 1-50 Hz



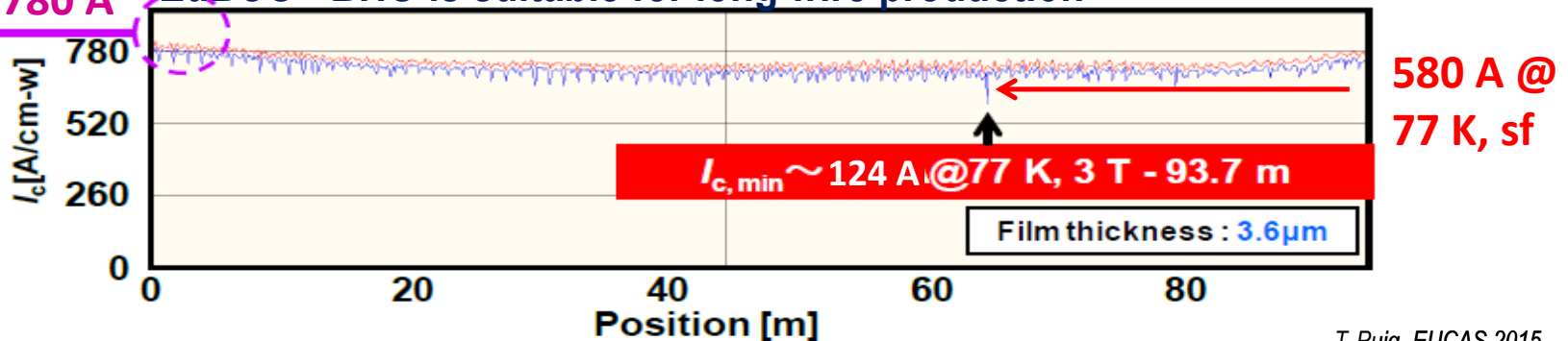
Very effective at intermediate T

EuBa₂Cu₃O₇ + BaHfO₃ by PLD has superior properties and it is scalable

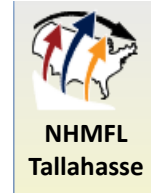


T. Yoshida et al, Physica C 504 (2014)

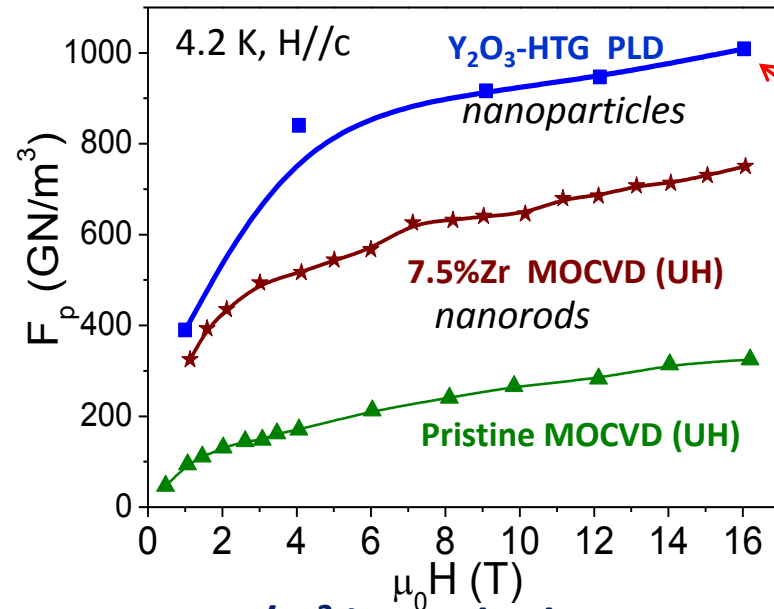
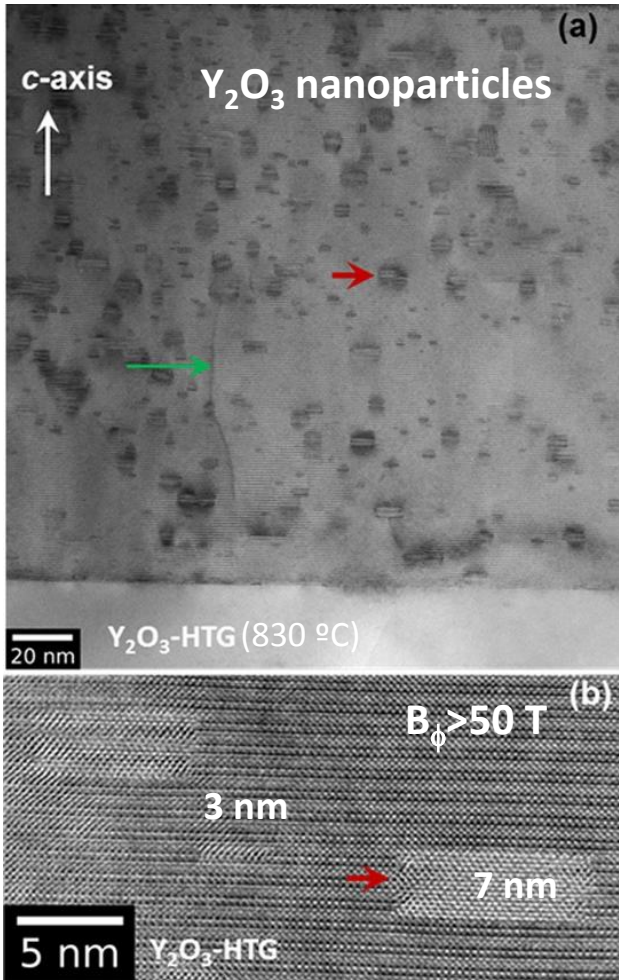
780 A EuBCO + BHO is suitable for long wire production



T. Puig -EUCAS 2015



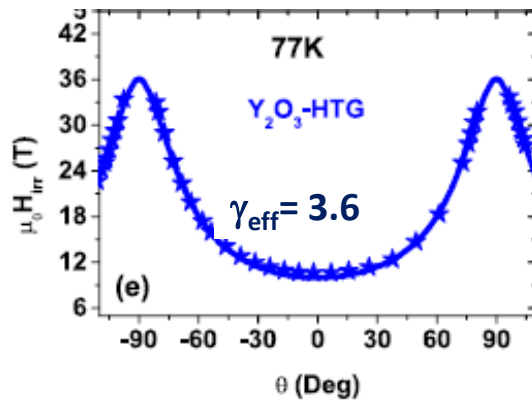
High F_p in YBCO PLD with Y_2O_3 nanoparticles



$J_c = 6,5$
MA/cm²

$F_p = 1000 \text{ GN/m}^3$ is reached at 4.2 K, 16 T

(Ni-Ti at 16.5 GN/m³)



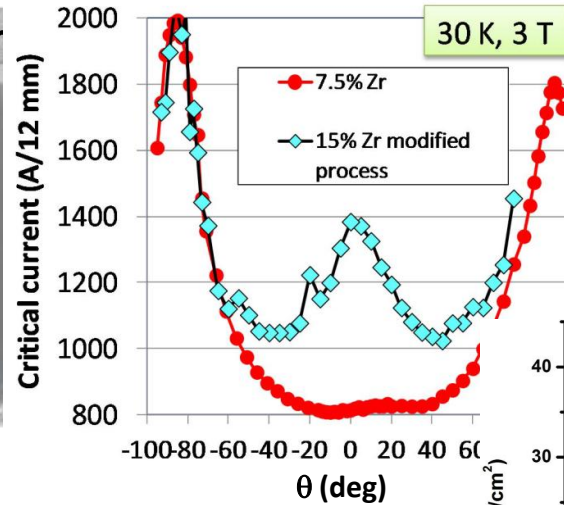
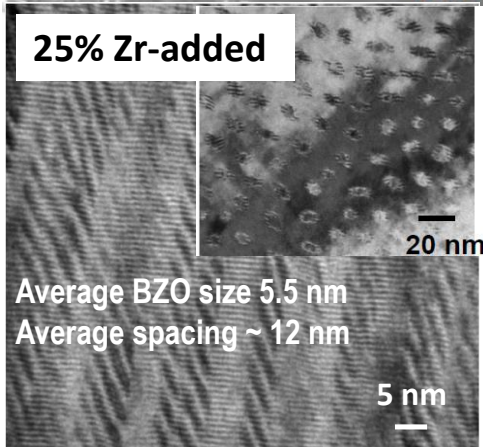
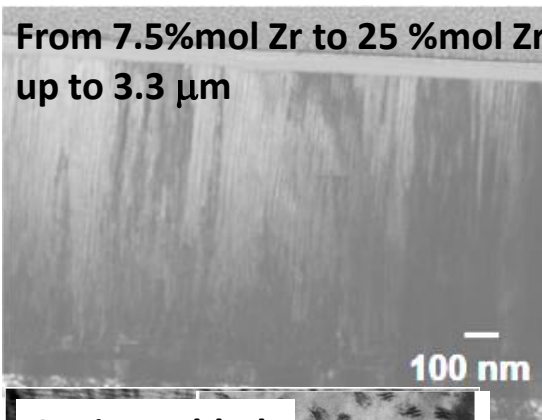
Isotropic strain pinning induced at low T

Reduced pinning anisotropy but $\gamma = H_{c2}^{ab}/H_{c2}^c = 5-7$

The Breakthroughs of Nanocomposites by MOCVD

A chemical vapor phase growth method giving rise to a self-assembly process of nanocolumns through spontaneous phase segregation

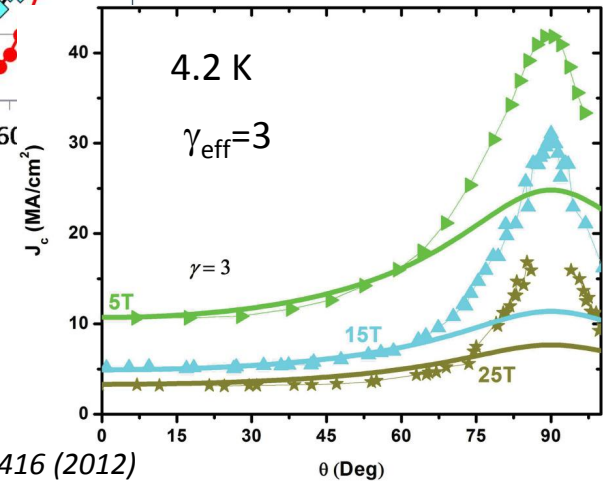
(Y,Gd)BCO –BZO with extrem high density of BZO nanorods



Anisotropic pinning from BZO nanorods dominates J_c down to 30 K

$F_p = 1650 \text{ GN/m}^3 @ 4.2 \text{ K}, 30 \text{ T}$

Weak Isotropic pinning strain field around BZO nanorods dominates J_c at low T



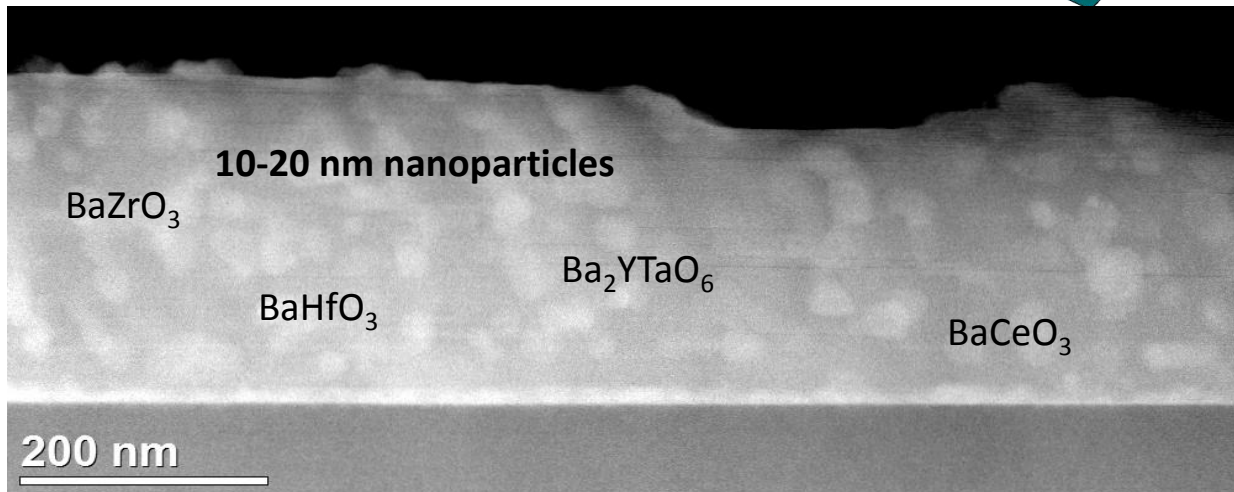
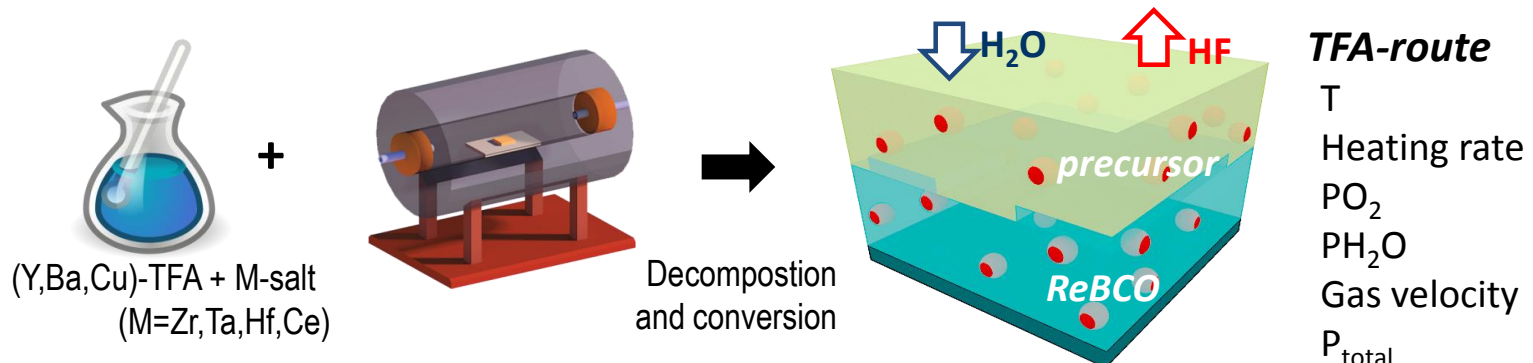
SUST, 26, 035006 (2013), PRB 86, 115416 (2012)
 APL MAT. 2, 046111 (2014)

T. Puig -EUCAS 2015

The Breakthroughs of Nanocomposites by Chemical Solution Deposition



A chemical gas-solid reaction growth method giving rise to a self-assembly process of nanoparticles through spontaneous phase segregation

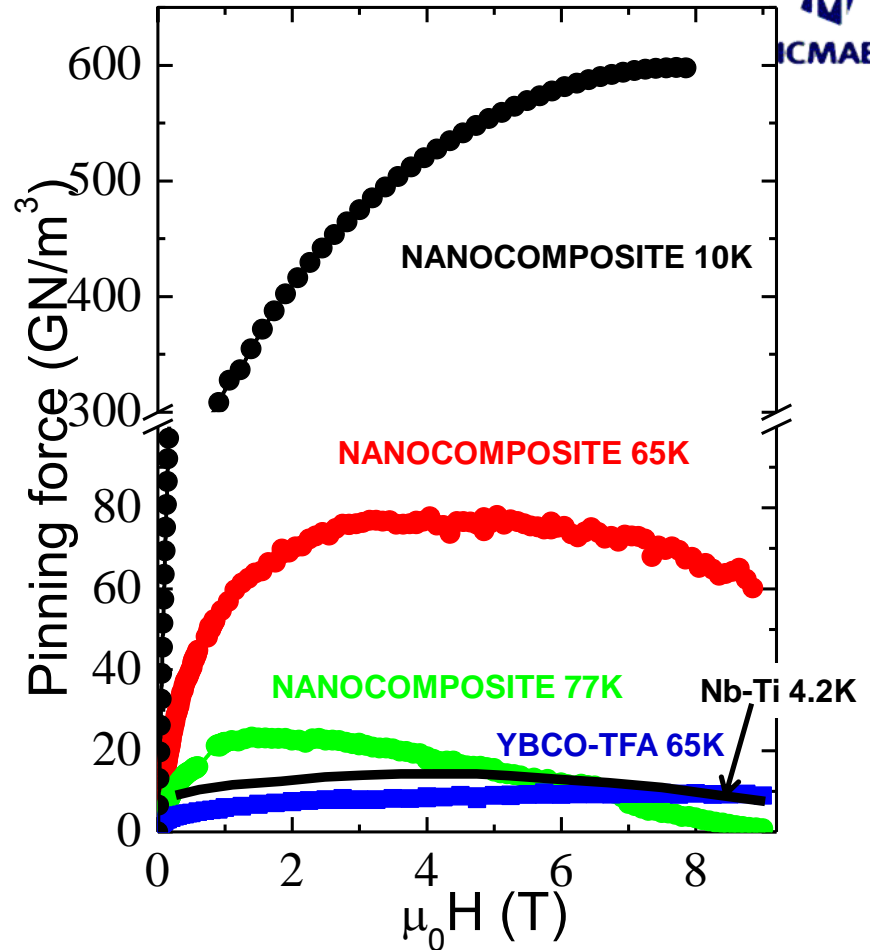
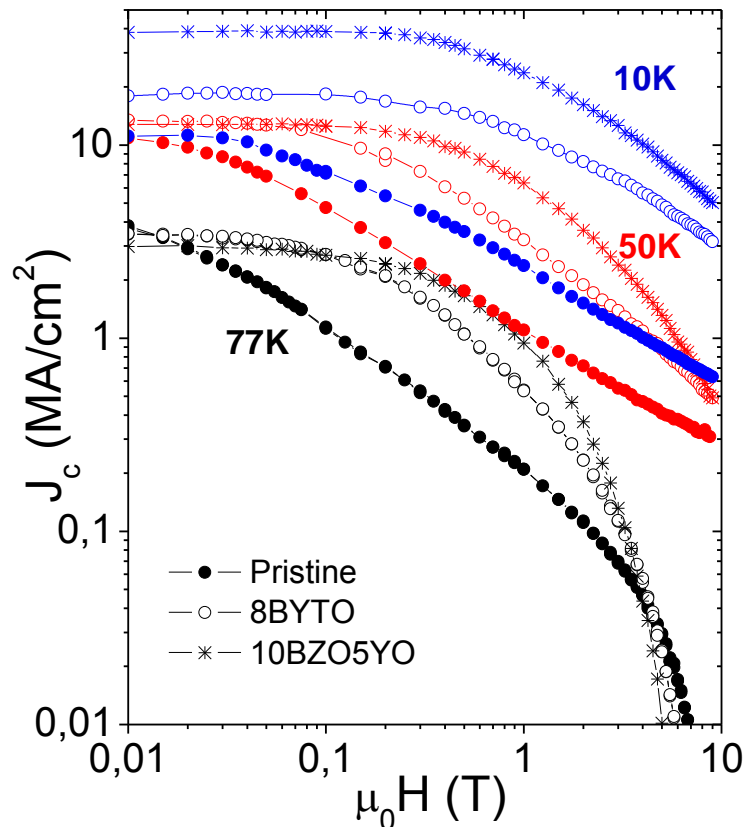


Randomly oriented nanoparticles are segregated from the YBCO matrix

High performance of CSD-YBCO Nanocomposites



High performance at all temperatures

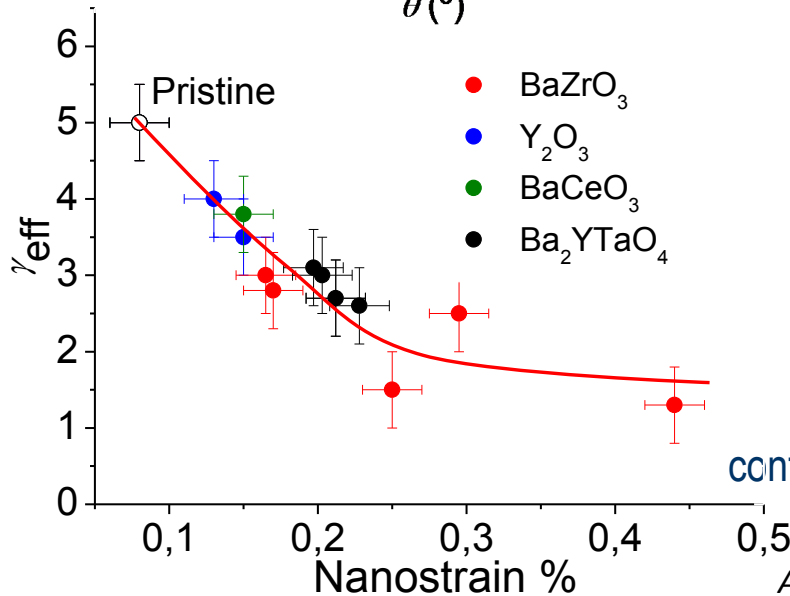
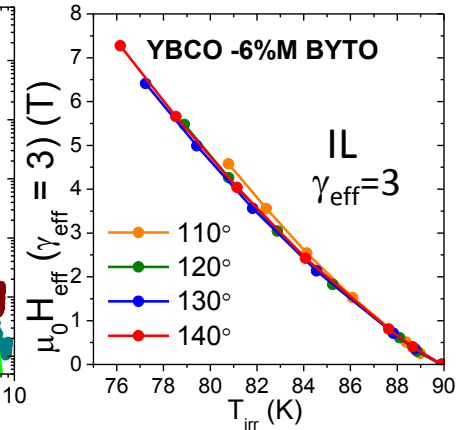
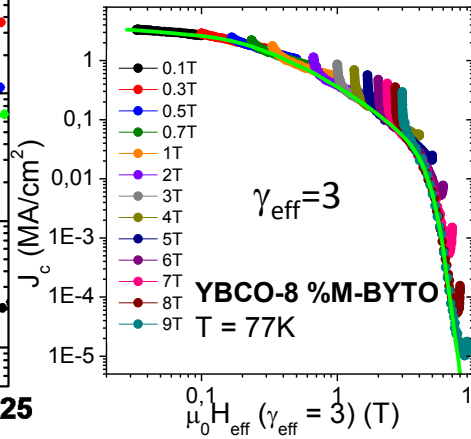
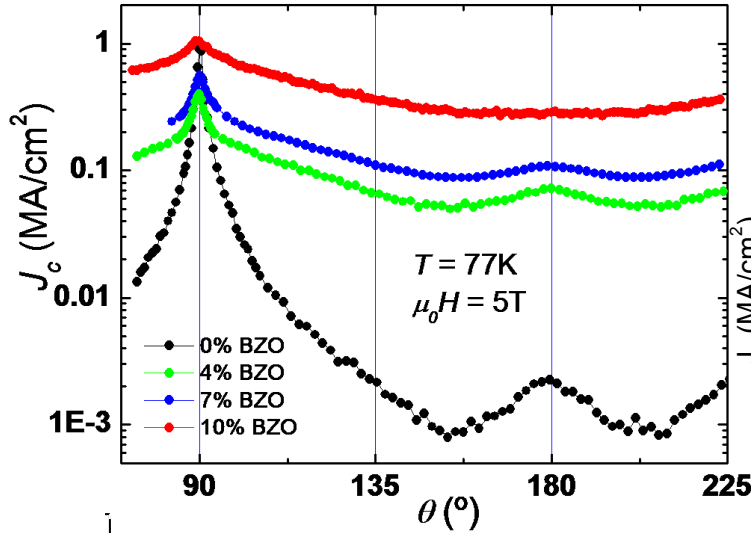


A. Llordés, et al. Nat. Mater, 11, 329 (2012),
J. Gutierrez et al, Nat. Mater. 6, 367 (2007)

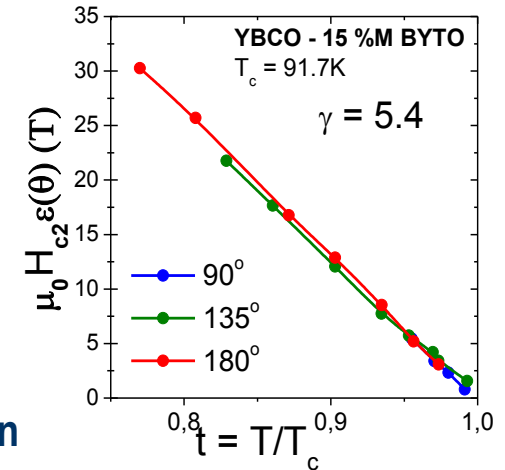
T. Puig -EUCAS 2015



Anisotropy in CSD Nanocomposites

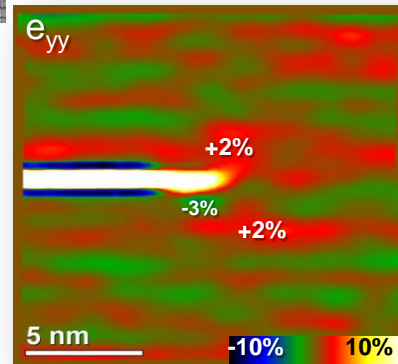
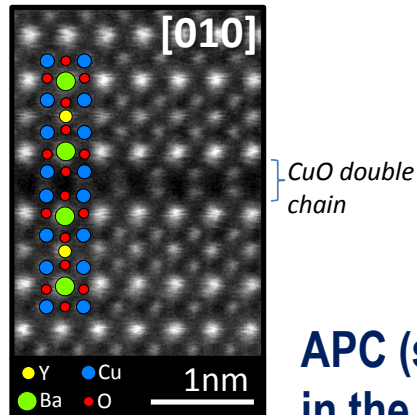
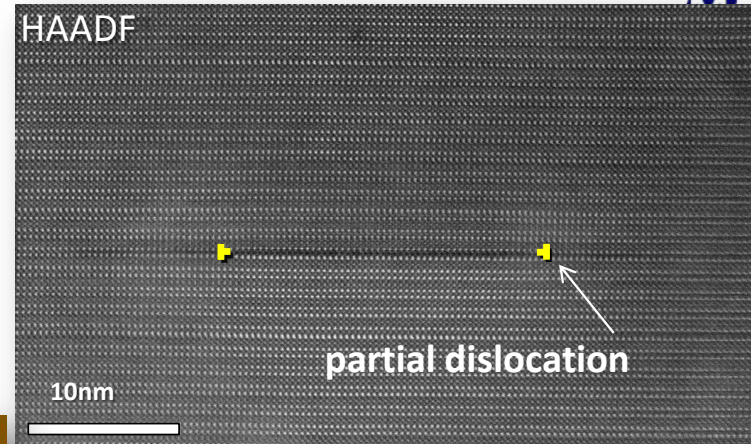
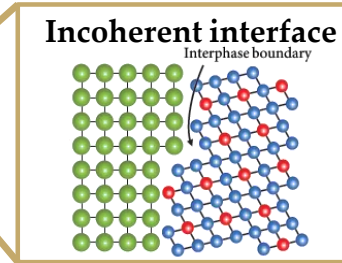
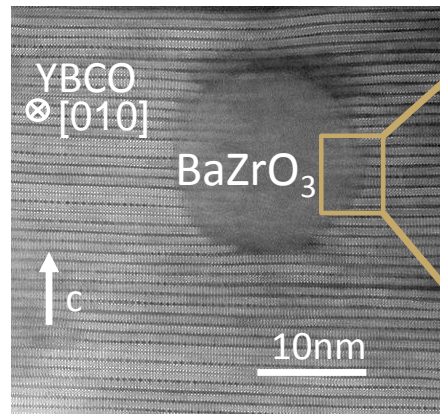


γ_{eff} reduction is controlled by nanostrain

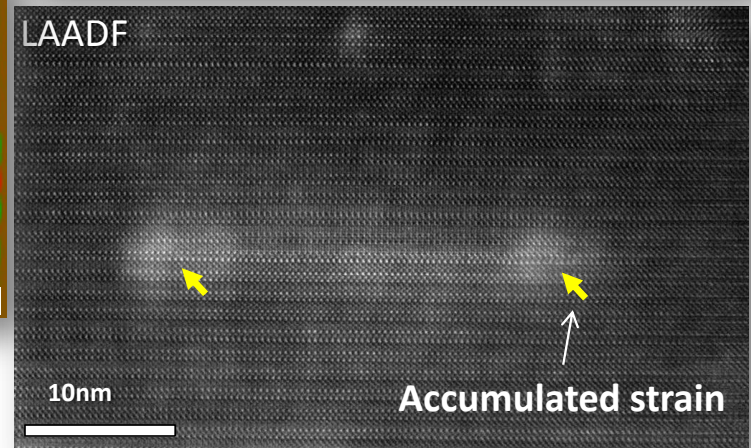




Incoherent YBCO-BaZrO₃ interfaces give rise to high density of Y248 intergrowths and associated nanostrain



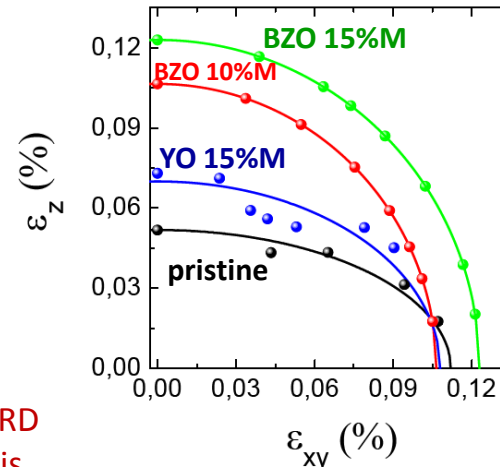
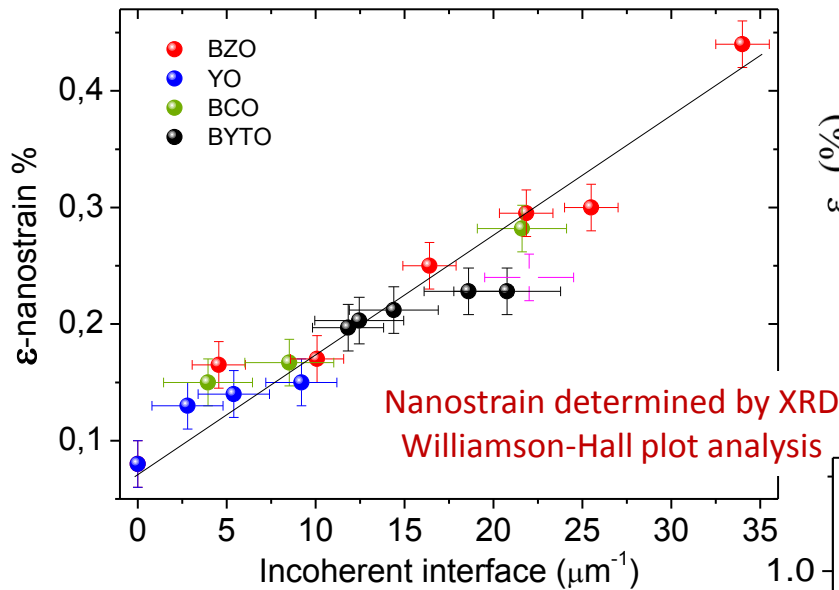
APC (strain) is embedded in the YBCO matrix



Local lattice strains control the isotropic pinning landscape of CSD-nanocomposites

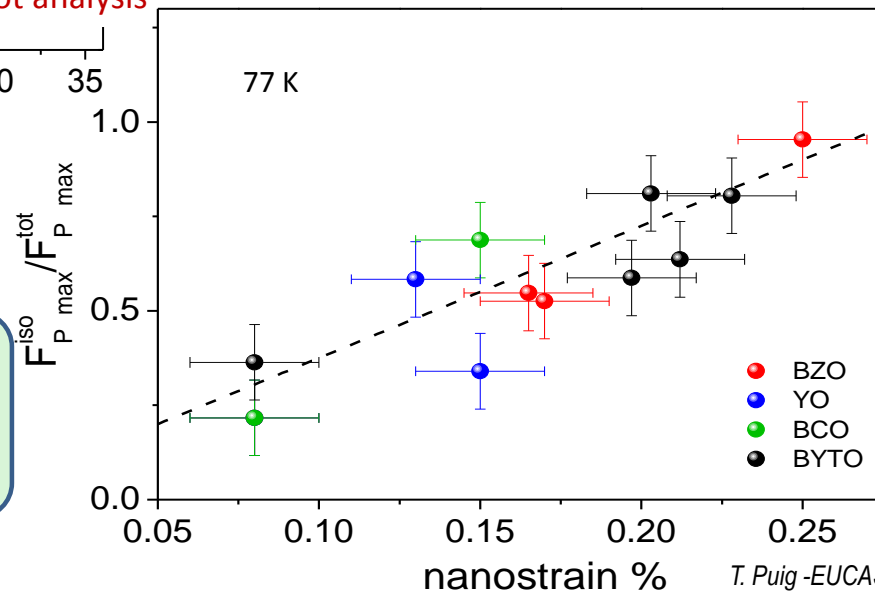


Random nanoparticles induce isotropic nanostrain



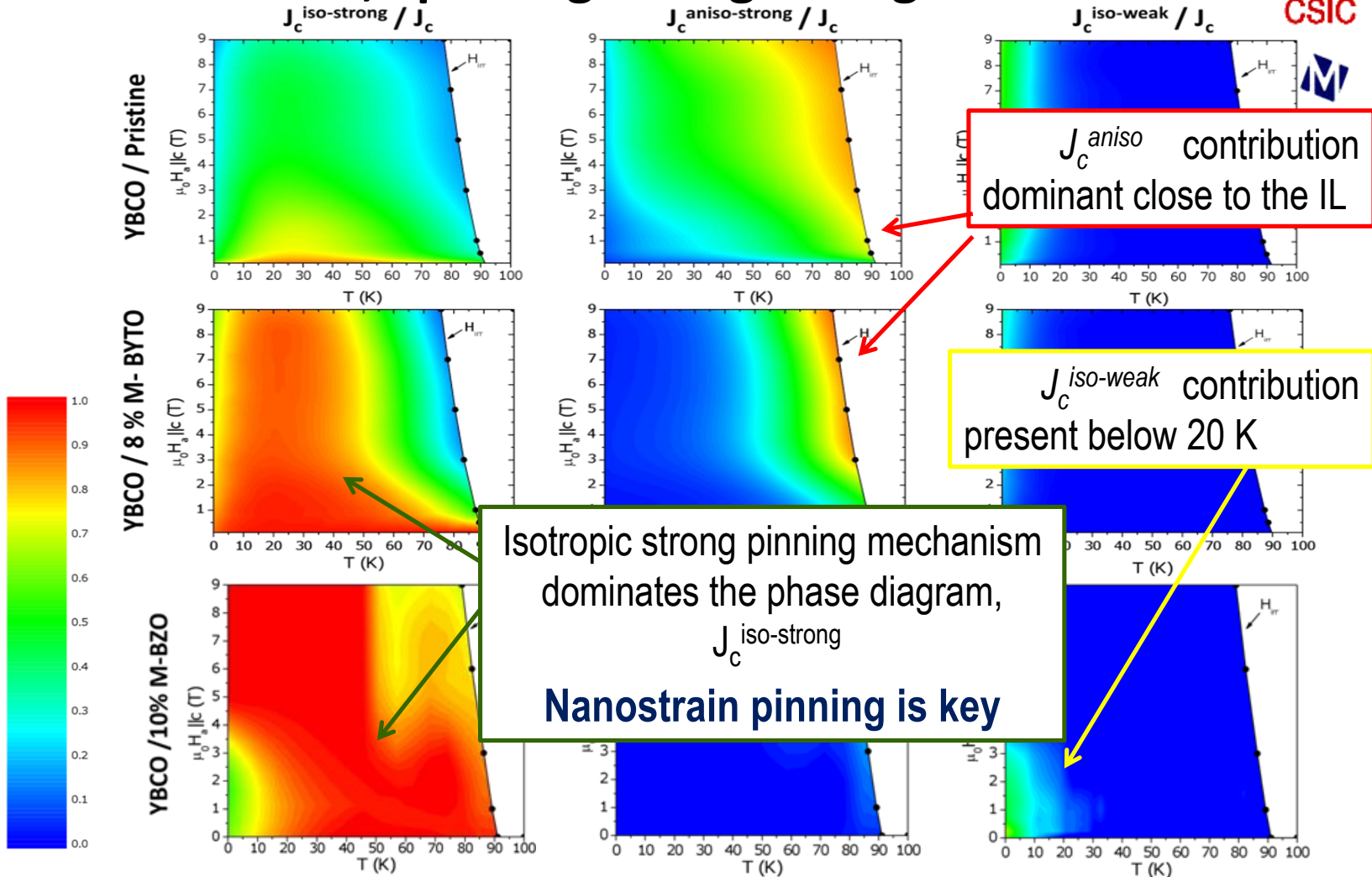
Nanostrain is controlled by random nanoparticles

The highest isotropic performance ever found in any superconducting material



Pinning properties of CSD YBCO nanocomposites

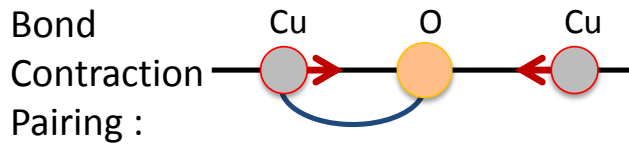
H,T pinning strength diagrams



T.Puig et al., SUST 21 (2008); J. Plain et al, PRB 65, (2002); J.Gutierrez et al., Appl. Phys. Lett. 90 (2007) T. Puig -EUCAS 2015

New vortex pinning mechanism based on strain induced Cooper-pair suppression

Nanostrain leads to unpaired nanoscale regions



Pair breaking energy:

$$2\Delta = 4 \frac{(t_{CuO})^2}{U} - 8t_0$$

$t_{CuO} (\propto 1/d_{CuO}^5)$

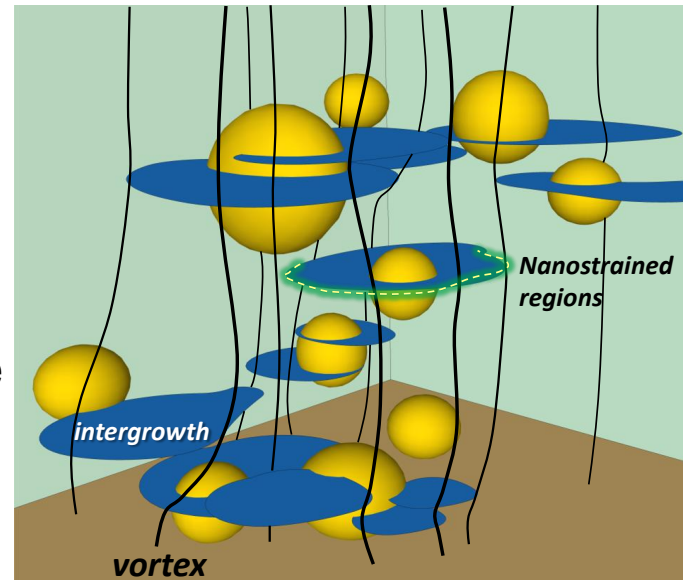
- t_{CuO} : transfer integral between Cu d and O p orbitals
- U : on-site Coulomb repulsion
- t_0 : half bandwidth

G. Deutscher, APL (2010)
Llordes et al., Nat. Mater 2012

Tensile strain quenches pair formation

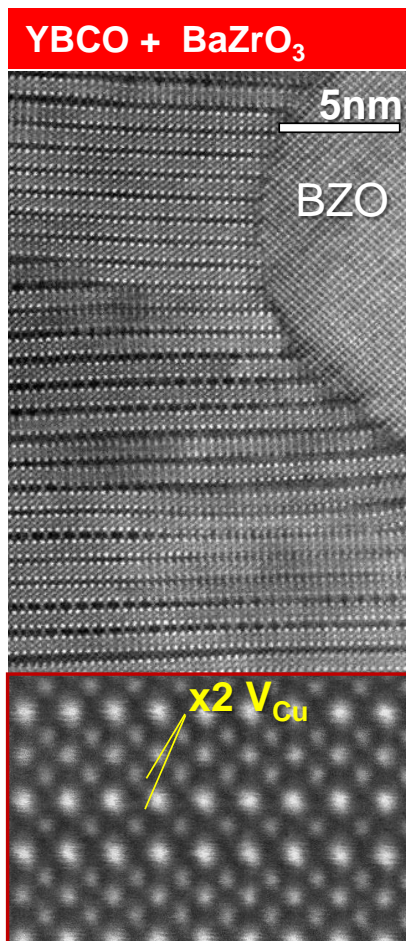
Vortex bending accommodates to a **3D ramified network** of localized isotropic nano-strained regions

Isotropic Strong pinning occurs by saving vortex line tension energy in a significant fraction of their length

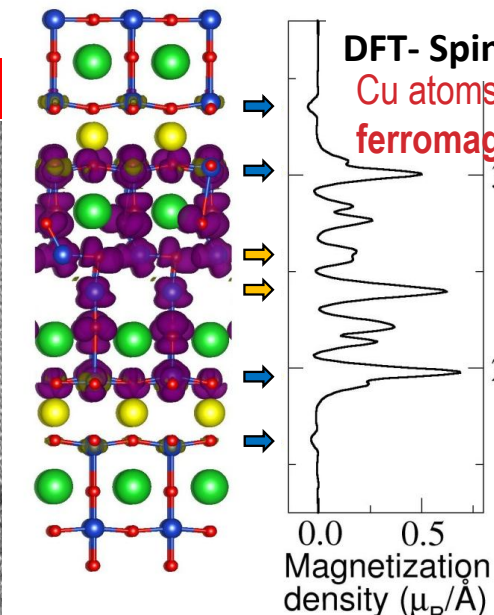


T. Puig -EUCAS 2015

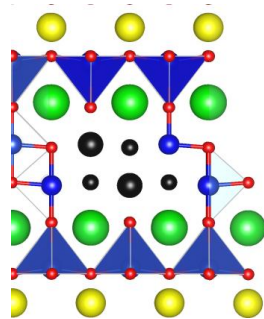
Vacancies in Y248 intergrowth avoid Stoichiometry Catastrophe



J. Gázquez et al, (submitted)



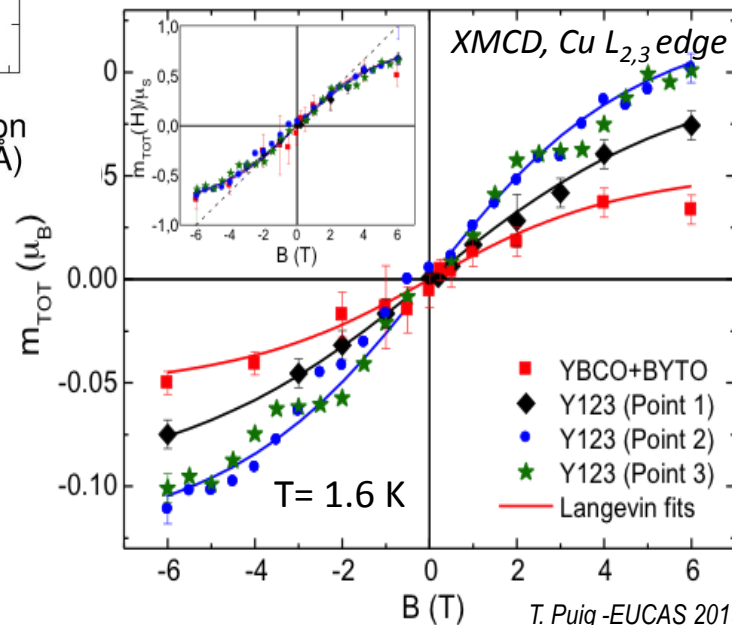
DFT calculations



$E/Cu=1.1 \text{ eV}$



This clusters induce dilute ferromagnetism in YBCO nanocomposites

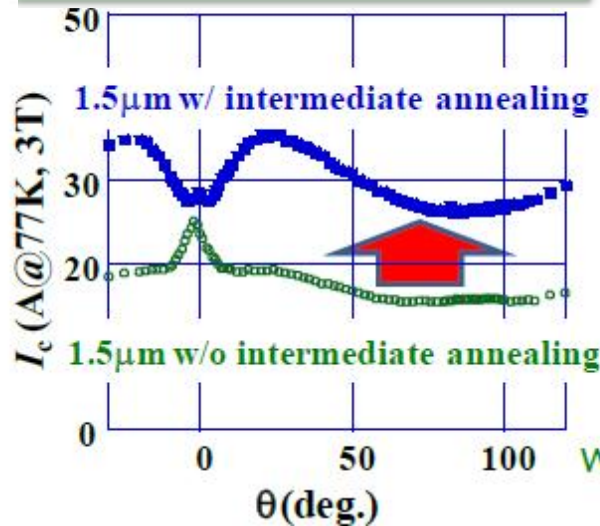
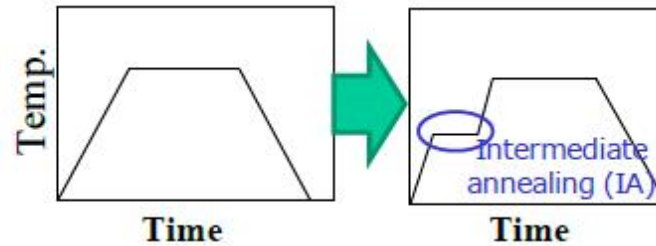
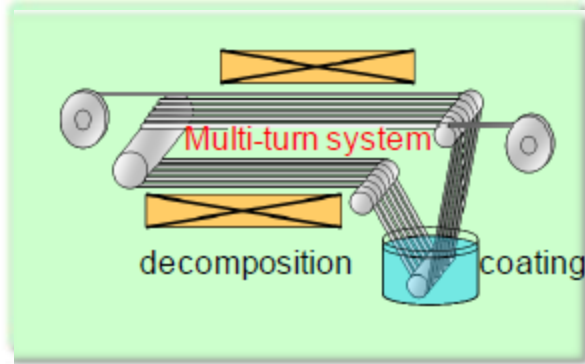


T. Puig -EUCAS 2015

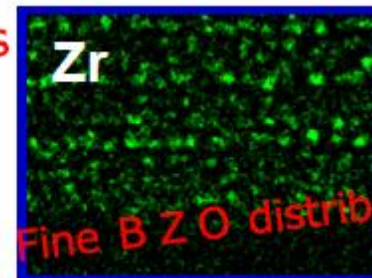
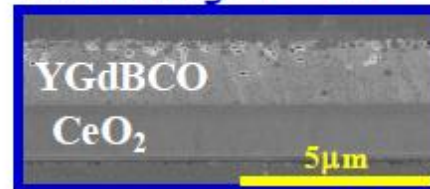


Nanocomposites by Chemical Solution Deposition : (Y,Gd)BCO+BZO

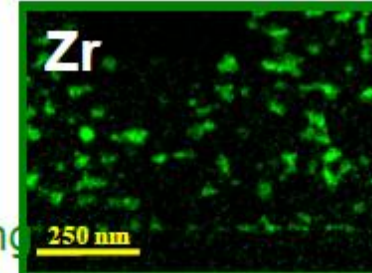
Improving in-field performance by limiting coarsening and avoiding porosity in thick films by an interim processes



w/ intermediate annealing **Less pores**



Fine BZO distribution

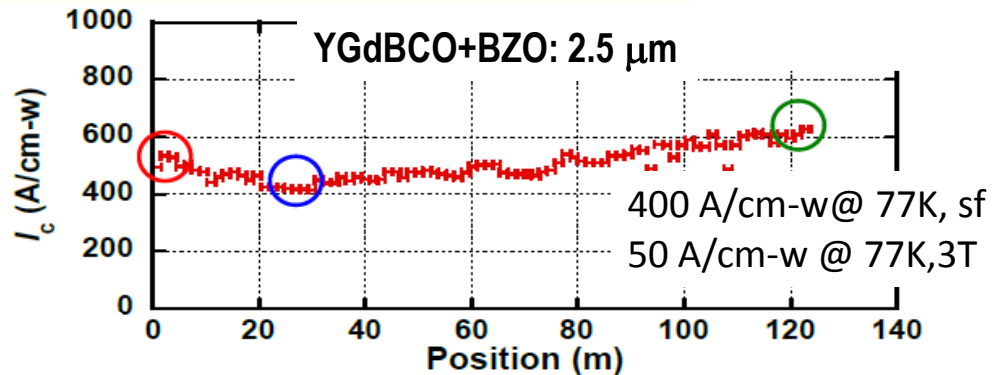
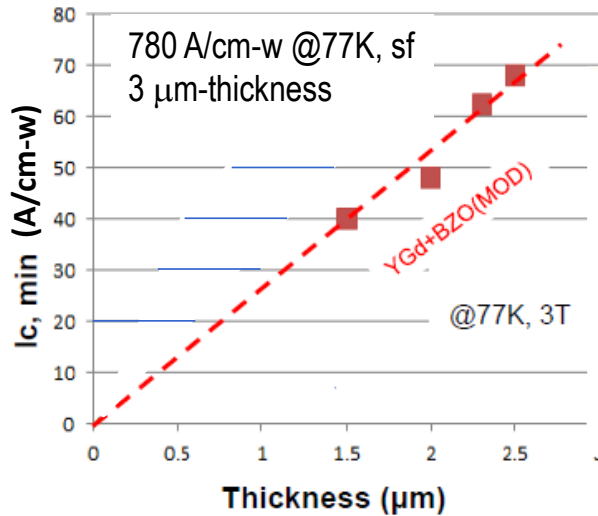


w/o intermediate annealing

Also at ICMAB M. Coll et al, SUST (2014)

T. Puig -EUCAS 2015

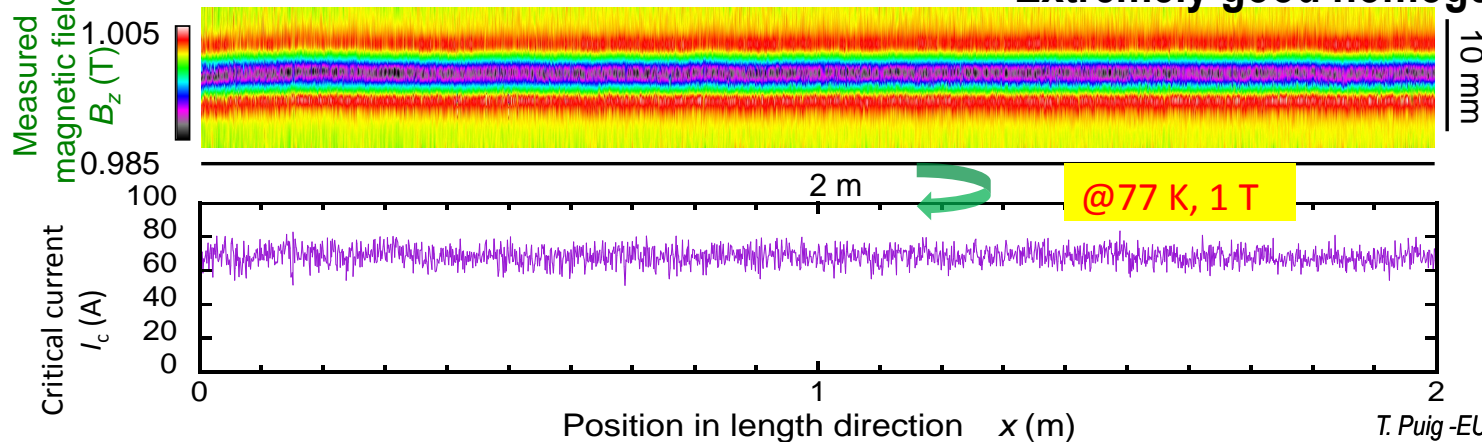
In-Field and Temperature dependence of (Y,Gd)BCO+BZO



CSD nanocomposites are scalable

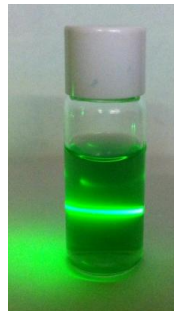
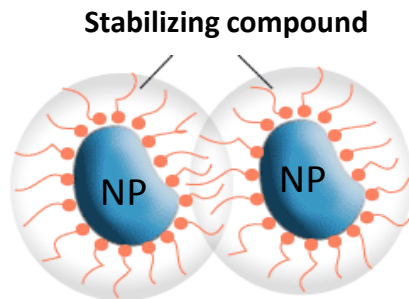
Scanning Hall Microscopy at 1 T

Extremely good homogeneity



T. Puig -EUCAS 2015

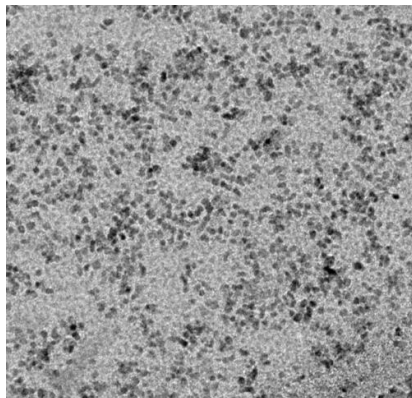
Nanocomposites by Chemical Solution Deposition with preformed nanoparticles



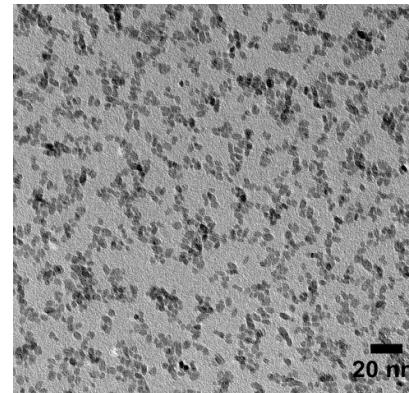
YBCO-TFA+ZrO₂ Np

Thermal and microwave-assisted solvothermal synthesis of nanoparticles

ZrO₂ Np(8x2 nm) in YBCO-TFA solution



CeO₂ Np(2 ± 0.4 nm) in YBCO-TFA solution



Several **oxide nanoparticles** could to be **stabilized in alcoholic and ionic environment** of YBCO precursor solution **at high concentrations**

P. Cayado, K De Keukeleere, et al SUST (submitted), F. Martinez-Julian, T. Puig et al. J. Nanosc. & Nanotech. 11 (2011)

I. Bretos et al, J. Mat. Chem. C 3 (2015), K. De Keukeleere et al, Inorg. Chem. 54 (2015)

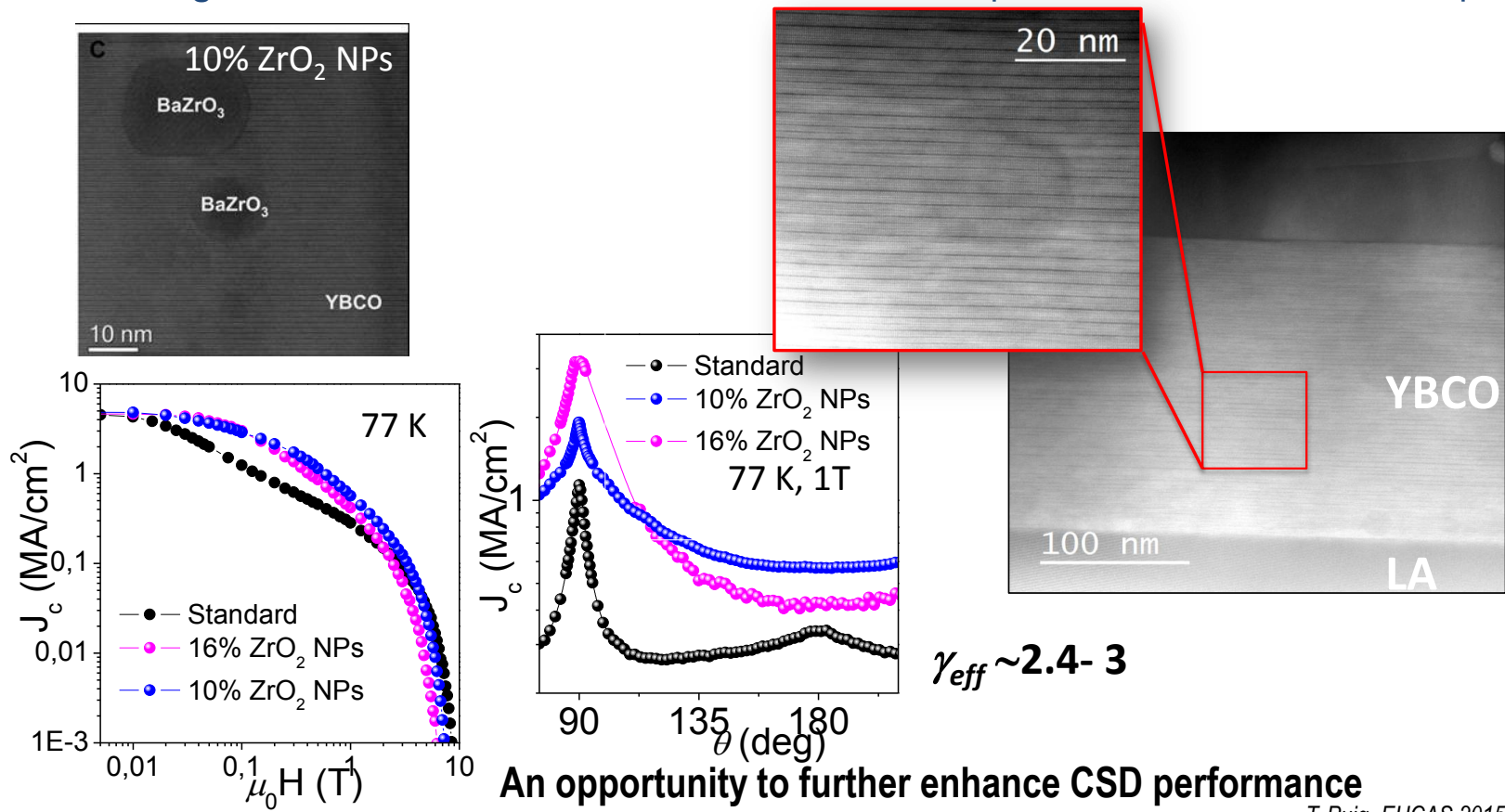
T. Puig -EUCAS 2015



CSD growth of Nanocomposites with preformed nanoparticles



Growth of **colloidal solutions** tend to induce **nanoparticles reactivity, pushing, coarsening** or **accumulation** at the substrate interface, but performance starts to show up



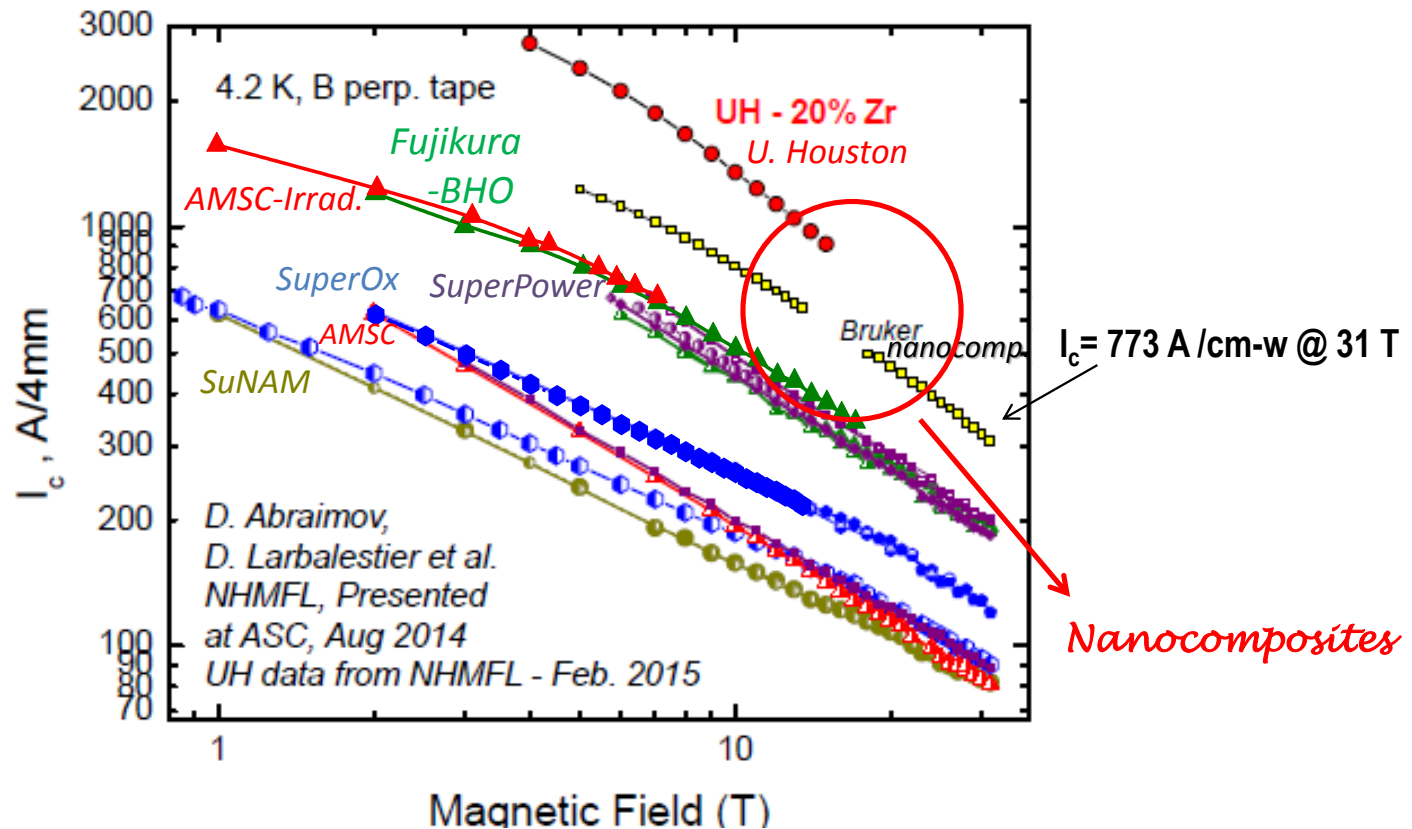
$\gamma_{eff} \sim 2.4 - 3$

An opportunity to further enhance CSD performance

Nanocomposite Coated Conductors

A reality and yet continuously improving

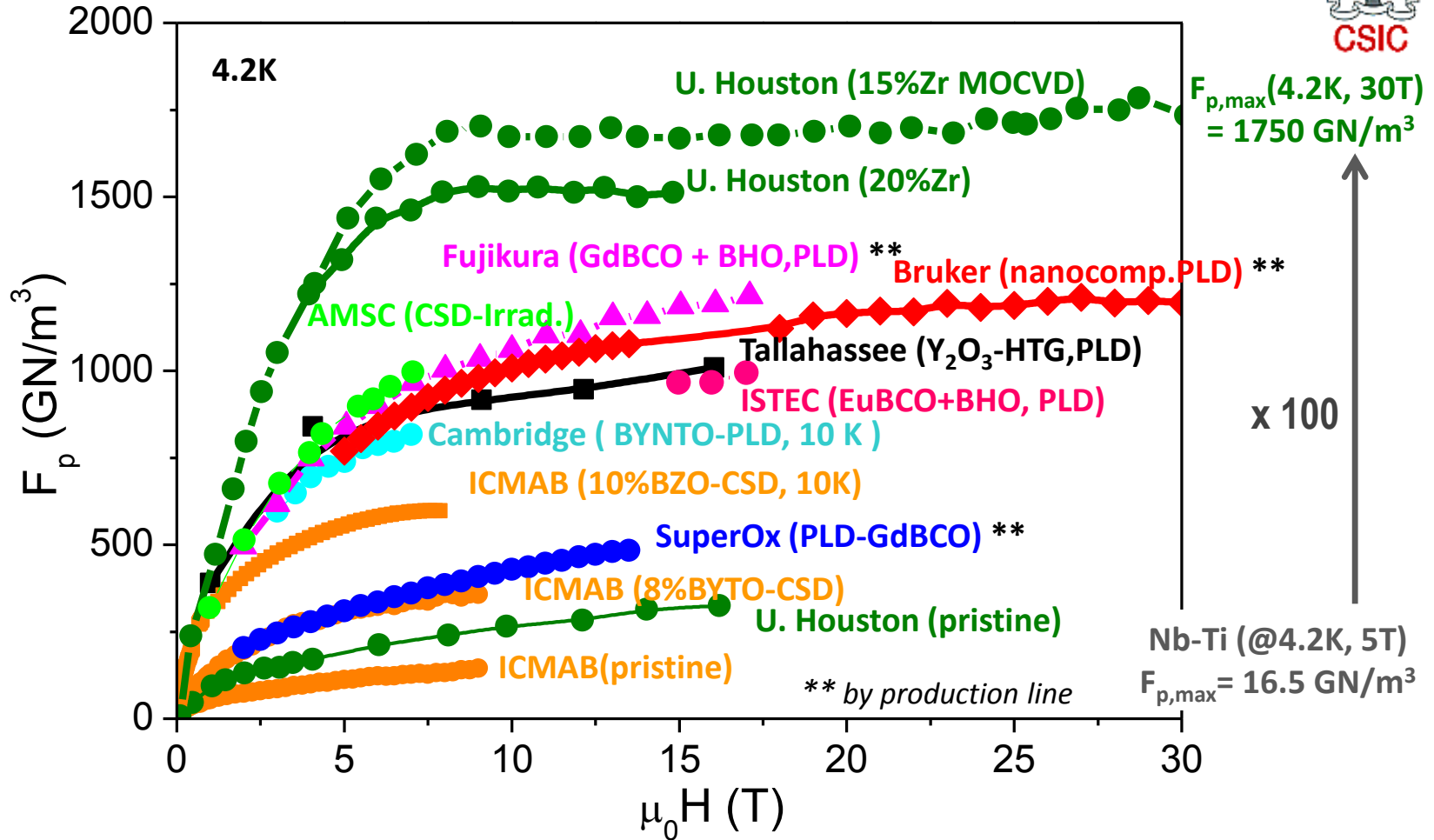
Now, strong interest for low temperature properties and ultrahigh magnetic fields



Courtesy of V. Selvamanickam -adapted

T. Puig -EUCAS 2015

Extraordinary future for ultra-high field applications



Isotropic (random) strain seems to be a common feature for increasing properties at low temperature and reach ultrahigh fields with nanocomposites

CONCLUSIONS



- **We are ready for HIGH FIELD CONDUCTORS development and optimization based on Nanocomposite Coated conductors (NCCs)**
- We should concentrate effort on **vortex pinning at 4.2 K**
- **HTS must join LTS efforts**
- NCCs are **scalable based on “react and wind”**
- Reinforce **fast and low cost growth** methods
- **Expanding manufacturing capabilities will decrease cost (Figure of merit €/kA-m @ H,T)**
- **R&D in technology issues beyond Critical Current:**
Compactness, transposition, quench detection, protection, joints, insulation, mechanical strength, ...

A winning story of joint efforts

**Materials Engineers, Physicists, Chemists, Electrical Engineers,
Manufacturers: The Superconducting Community**